NAIST-IS-DD0661015

Doctoral Dissertation

Studies on Kinetic Human-Machine Interaction Using User's Biological Signals

Tomoya Tamei

February 5, 2009

Department of Bioinformatics and Genomics
Graduate School of Information Science
Nara Institute of Science and Technology

A Doctoral Dissertation
submitted to Graduate School of Information Science,
Nara Institute of Science and Technology
in partial fulfillment of the requirements for the degree of
Doctor of ENGINEERING

Tomoya Tamei

Thesis Committee:

Professor Kazushi Ikeda	(Supervisor)
Professor Tsukasa Ogasawara	(Co-supervisor)
Associate Professor Tomohiro Shibata	(Co-supervisor)

Studies on Kinetic Human-Machine Interaction Using User's Biological Signals*

Tomoya Tamei

Abstract

In this dissertation, I propose a realization of the kinetic interaction between a user and a machine using his/her biological signals such as motion and surface electromyogram (EMG) signals. A surface EMG signal is a temporal and spatial summation of action potentials generated by motor units (MU) and thus has a casual relationship with muscle activities. The surface EMG signal can be measured noninvasively with relative ease and reflect voluntary signals from the central nervous system prior to muscle contractions. Consequently it has been utilized in various fields such as neurophysiology, clinical medicine and sports science/engineering. In recent years EMG technology has become less expensive and measurement devices have improved in performance. Consequently, EMG-based applications such as power assist, prostheses and operational interfaces are now being extensively studied. Since most existing applications generally have degrees-of-freedom (DOF) limitations in sensing as well as movement, there is a need to improve the performance of these applications for use in the real world. Therefore, in this study, I propose an approach which can realize the kinetic interaction with machines by estimating force/tactile senses in real-time from the information obtained from noninvasive measurement devices, that is, EMG measurement and motion capturing devices.

This study first proposes a new approach to designing intelligent machines which is a virtual realization of force/tactile sensors in machines equipped with no real sensors. Because this approach does not require any sensor attached to a robot, it can also be applied in principle to various other machines. To investigate the feasibility

*Doctoral Dissertation, Department of Bioinformatics and Genomics, Graduate School of Information Science, Nara Institute of Science and Technology, NAIST-IS-DD0661015, February 5, 2009.

of this approach, I constructed an experimental system which consisted of a robot, a surface electromyograph and an optical motion capture device. The kinetic and intuitive interactions were achieved by estimating the force exerted by a user at the point of action in real-time and from the user's motion information and EMG signals. As a realistic cooperative exercise, the task of cooperatively holding and moving a heavy load vertically was conducted and successful results were obtained.

Next, I attempted to expand the above cooperative holding task to a three-dimensional version. However, the conventional method in which the parameters of the estimator should be trained in advance did not work due to the changes in the EMG signals which were attributed to time variations in the muscle coordination patterns. To overcome the difficulty, I introduced a reinforcement learning process which modifies the policy function based on the user's biological signals. The benefits of the reinforcement learning process are: (1) the parameters of the estimator can be adjusted on-line during the task, and (2) it can be applied without any explicit teacher signal such as a force sensor output (it can be applied to the robot that possesses no sensors). In addition, the reinforcement learning based on the user's biological signals should adaptively assist the motor learning system to achieve the desired outcome for the user.

Keywords:

human-machine interaction, force/tactile sensing, electromyogram, motion capturing, reinforcement learning

ユーザーの生体情報を用いた機械との動的インタラクションに関する研究*

爲井 智也

内容梗概

本論文の目的は，ユーザーのモーション・表面筋電信号といった生体情報を用いた，機械との動的なインタラクションの実現を提案することである．表面筋電信号とは，皮膚表面で計測される筋活動に因果関係のある電位で，運動単位（MU: Motor Unit）の活動電位を時間的・空間的に重ね合わせたものにあたる．中枢神経からの随意信号を非侵襲で比較的容易に記録できることから，従来から神経生理学や臨床医学，スポーツ工学といった分野で計測・解析が行われてきた．先に述べたように筋電は運動の原因である脳からの運動指令を含むため，筋肉の収縮よりも先に観測することができる．これに加え，近年では計測機器の性能の向上や普及化といった要素も後押しし，筋電を利用したパワーアシストや義手，機器操作デバイス等のヒューマンインターフェースの研究が盛んに行われるようになった．しかし，運動に用いる部位を著しく限定したものや運動範囲を平面に拘束したもの，静的運動時の使用に限ったものが多く，動的な運動時における使用や運動空間の制約という点では実社会での使用に向けて向上の余地が多く残されている．そこで本論文では，筋電計測装置とモーションキャプチャという二つの非侵襲計測機器の情報からユーザーの力覚や触覚を実時間で推定することにより，機械とのインタラクションを実現する方法を提案する．

まず，ユーザーの生体情報をリアルタイムで通信することにより，センサを持たない機械に仮想的な力覚・触覚を持たせる新しい知能機械の設計アプローチを提案した．本アプローチは制御対象に依存しないため，幅広いロボット・機械に適用することができる． 本アプローチの有用性を検証するために，センサを持たない産業用ロボットマニピュレータ，表面筋電（EMG）計測装置，モーショ

*奈良先端科学技術大学院大学 情報科学研究科 情報生命科学専攻 博士論文, NAIST-IS-DD0661015, 2009年2月5日.

ンキャプチャーシステムからなるシステムを構築して実験を行った．ユーザーのEMG と姿勢情報からリアルタイムでユーザーの発揮した手先の力を推定することでロボットに力覚／触覚を持たせ，直感的かつ動的なインタラクションを実現した．更に，応用例としてユーザーとロボットが協調して鉛直方向への重量物の持ち上げ・下げ作業を行うタスクも実現した．

次に，ユーザーとロボットによる重量物の協調把持作業の 3 次元への拡張を試みた．しかし，タスクの前に推定器のパラメータを学習しておくという従来の方法では，筋肉の協調パターンの時間変化による EMG 値の変化により，タスク時には推定精度が著しく悪化してしまう．この問題を解決するため，ユーザーの生体情報に応じて方策関数を改善する強化学習の導入を提案した．強化学習を用いることによって,（１）タスクを行いながらオンラインで推定器のパラメータの調整が可能である,（２）センサの出力等の明示的な教師信号がなくても学習（センサを持たないロボットへの適用）が可能である，という利点がある．また，生体情報を用いた強化学習は，将来的に，ユーザーの意図や運動能力，個性に合わせて適応的にアシストを行う運動学習支援システムへの応用が期待される．

キーワード

マンマシンインタラクション, 力覚／触覚, 筋電図, モーションキャプチャ, 強化学習

Contents

List of Figures

List of Tables

1. Introduction

There is an increasing potential market for robots that can provide home-help in an environment where there is an aging population combined with a diminishing number of children. Such robots are required to possess not only visual and auditory perception but also force and tactile sensors which achieve dynamic and cooperative interactions with their users. If this technology is successful, the human affinity for welfare, livelihood-support and entertainment robots could be greatly increased. In addition, if it is applied to the teaching of industrial robots operating in factories, of the ability to perform complex motions could be easier.

Typically force/tactile sensors have been designed to be mounted over the robot's body (e.g., [49, 26]). The use of such an approach, however, is generally limited because of low spatial resolution, small degrees of freedom (DOF) of each sensor, complicated wiring, the necessity for repairs, and so on. Recently, in the search for realistic ways of designing intelligent robots, the trend has been towards completely autonomous and self-contained sensor robots as well as attempts to place many sensors in the environment [50, 31]. These robots could obtain a wide range of sensory/perceptive information in their operating environment.

The aim of this study is to control a robot (as an example of machines) by means of a user's biological signals, and to realize dynamic and intuitive interactions between a robot and a user. The most important key to my approach is that the robot expands its sensing ability by receiving the user's biological signals in real time. I particularly focused on electromyogram (EMG) and motion information as biological signals for this purpose. EMG signals reflect motor commands from the brain for muscle contraction, and many processing methods and applications have been proposed [15, 60, 56]. Previous studies showed the possibilities of estimation of joint torques, stiffness, and the trajectory of an elbow and a shoulder, using EMG and motion signals [33, 34]. Such information, estimated from the user's biological signals, can be used by the robot as its own force senses. Since the rise of EMG signals is observed prior to actual movements, employing EMG signals allows a robot to interact with a user under delay-compensated control, leading to natural interaction with the user. Furthermore, the use of EMG seems realistic; since biological signal measurements including EMG are still maturing, and measurement will become less expensive and easy in the near future. Additionally, a technique based on a noninvasive measurement is inherently

safe.

On the other hand, EMG applications have several difficulties. EMG can be influenced by many unpredictable factors which are physiological and nonphysiological ones such as crosstalk among nearby muscles, pattern changes of EMG due to muscle coordination or skin-electrode contact [15, 20, 60, 16]. To realize practical interaction between a user and a machine using user's EMG signals, a way to deal with these difficulties is needed.

1.1 The EMG process

Muscle activation occurs from a combination of some muscle fibers supplied by signals from the central nervous system (CNS) via a motor nerve. This combination of muscle fibers and a motor nerve is called a motor unit (MU). Motor nerve excitation reaches the motor end-plate via a motor nerve as an impulse train, and then the muscle fibers start contracting with the electrophysiological depolarization of its membrane. Surface EMG is the method for recording signals with the spatial and temporal superposition of motor unit action potentials (MUAPs) by electrodes attached to the skin on the upper layer of the target muscle. It has the advantage that it is a noninvasive and relatively easy way to record the activities of CNS. Therefore, it have been measured and analysed in various fields such as neurophysiology, clinical medicine and sports science/engineering [4, 22, 47, 75]. EMG signals can contain information such as muscular effort and fatigue. This information was estimated mainly from signal amplitude and frequency. There have been evaluation indices of EMG, and muscle effort and fatigue was estimated mainly from signal amplitude and frequency [59, 36, 53, 18], respectively. Recently, muscle effort is often used for as an input to the controller of myoelectric devices like power-assist and prostheses [27, 74, 2].

1.2 Human-Machine Interfaces based on Surface EMG

There have previously been studies of Human-Machine interfaces based on surface EMG such as prostheses and power assists (e.g., [11, 32, 23, 54, 28, 1, 21]). Most previous studies estimate joint torque, hand trajectory or hand motion as a pattern intended to control a specific machine or device, however, the studies that estimate the force exerted by user's hand are less common [1]. In this study, for example, I can

give force/tactile senses to existing robots by estimating the force exerted by the user's hand.

This force, applied at the interfaces, can be estimated in two ways using either anatomical or physiological models [13, 43, 37, 45, 19] which provide a functional approximation with no knowledge of the underlying and controlling physical phenomena [35, 44, 42]. Each way has advantages and disadvantages. The model-based way which uses a muscle model such as Hill-based [25, 69] and musculoskeletal-model [8, 40]. These approach can handle a large variety of situations, because it is modeled from the muscle activated output force based on a knowledge of phenomenological analysis. However, since the formulation is complex it is impossible to estimate with high accuracy for the case of movements which incorporate many muscles and joints. Furthermore, the model parameters probably depend on user. It is usually necessary to normalize the EMG with maximum voluntary contractions (MVC) [70] to quantify muscle activation, because the amplitude of EMG often varied with the postural changes of the user and the positions of the attached electrodes [10]. Since each muscle activity is determined from certain EMG signal, The correct interpretation of the EMG is often questioned for the reasons described above. On the other hand, the functional approximation way is task dependent, because its parameters relied on training data, and a calibration procedure to obtain a mapping between input and output may be needed each time a subject is changed. The performance of the approximator tends to be affected by the time varying nature of the EMG signals and muscle coordination due to efficiency for the task and fatigue [39, 55, 6]. Although it is simple to apply and can indicate good performance for simple problems [57], the relationships between input and output are more complex and higher computational power is required and solutions are not possible in real-time. In fact, in real-time, either modeling method can only estimate the torque for two joint's which move in the same plane. We have not achieved estimation for the cases which have a wide range of movement or changes of velocity.

1.3 Organization of Dissertation

This dissertation is organized as follows. The next section proposes a new approach to realizing dynamic interactions by using user's biological signals, and then describes an experimental system to investigate the feasibility of my approach. Section 3 presents

four experiments demonstrating that an industrial robot manipulator can behave as if it had virtual force/tactile senses and can perform a cooperative exercise with its user. Section 4 first proposed to apply the reinforcement learning method to the VFS, and then describe its example application to the cooperative holding task, demonstrating the feasibility of my approach. Section 5 concludes this study with detailed discussions and recommendations for future research.

2. Kinetic Human-Machine Interaction

2.1 Kinetic Human-Machine Interaction

To establish the interface between humans and machines, it is necessary to estimate the information which reflect the user's intentions in real-time and to allow a variety of different motions. Although, most of previous studies of Human-Machine interfaces based on surface EMG are intended to control a specific machine or device, if the machine expands its sensing ability by receiving the user's biological signals, it makes it possible for the user to interact with many machines. This study proposes an approach to realize kinetic and intuitive interaction with machines by giving virtual force/tactile senses to machines equipped with no real sensors .

2.2 Virtual Realization of Force/Tactile Sensing

In this study, I propose a novel approach to virtual realization of force/tactile senses in robots (machines) which do not normally possess such sensors. Note that, in this article, "tactile sense" means the location information around the position at which force is applied but does not mean any textural information. The key factors to my approach are: (1) I restrict situations to those in which a robot interacts with its user, and (2) the robot expands its sensing ability by receiving the user's biological signals, such as the surface EMG and postural information in real time. The estimation methods of the force applied to the manipulator from eiher human or environment sources without using the force/torque sensor have been proposed [62, 51]. However, these methods require the accurate dynamics model of the robot. The higher the gear ratio of joints or the less their back-drivability becomes, the lower the force sensitivity gets. Therefore, it seems impractical to use these methods widely for human-robot interaction.

Table 1 shows the comparison of the approach proposed in this study with the other approaches that involve the sensors attached to a robot (real sensors) and those embedded in the environment (environment-integrated sensors). The real sensor approach allows a user to interact only with the robots in which sensors are mounted. On the other hand, because my approach does not require the sensors to be attached to a robot, it can be applied in principle to not only robots but also to various other machines. In other words, my approach has the possibility of enabling a user to interact with many

machines by using fewer sensors than the real-sensor approach. Furthermore, my approach has great advantages as it is highly general and very extensible. As an example of this, teleoperation is feasible by means of remotely sending biological signals to a robot. Force measurement can be carried out independently of the positions and types of sensors. Hence higher spatial resolution and the ability to cope with large DOFs can be realized rather easily. The real sensor approach has realized high spatial resolution by mounting sheet-like force sensors on a robot [49, 26]. However so far, this approach has performed only one DOF force measurement at a point. The environment-integrated approach uses various sensors embedded in the environment. For example, embedded cameras [31, 30] and a force sensing sheet [52] have been used. This approach is one promising way to develop intelligent systems, but also has the difficulty of increasing the number of spatial resolution and measurement DOFs for force/tactile sensing, compared to my proposed approach. My approach can rather easily achieve both high spatial resolution and measurement DOFs for force/tactile sensing in robots which do not possess such sensors, as will be demonstrated in this study. Furthermore, natural user interfaces could be realized by using the user's EMG signals, because the EMG signals reflect motor commands of the user's brain, and can be used to estimate muscle tension and joint stiffness. It should be noted, however, that my approach does not exclude the real-sensor and the environment-integrated approaches but is complementary to them. My approach will become more advantageous especially under the ever expanding ubiquitous computing environments in which sensors and devices are networked and are distributed over the environment. For instance, the problem that the robot cannot detect obstacles except its user could be solved by employing either external cameras or ultrasonic/touch sensors attached to the robot. Although the experimental setup described below is large and expensive, the ubiquitous computing environments will provide alternative methods and devices. Further discussions related to these comparisons will be presented in section 3.5.

2.2.1 Virtual Force Seinsing Procedure

Figure1 shows the comparison of force sensing process between my approach (VFS: Virtual Force Sensing) and real sensor approach. While real force sensing approach obtain the force by the force sensor attached on the machine, VFS approach estimates the force from user's biological signals such as motion and EMG which are obtained

Table 1. Comparison of approaches to force/tactile sensing for robots

	Real sensor	Environment-integrated	Proposed approach
Controlled object	limited	wide	wide
Teleoperation	impossible	possible	possible
Spacial resolution	low	low	high
Measurement DOF	low	low	high
Obstacle detection	possible	possible	impossible

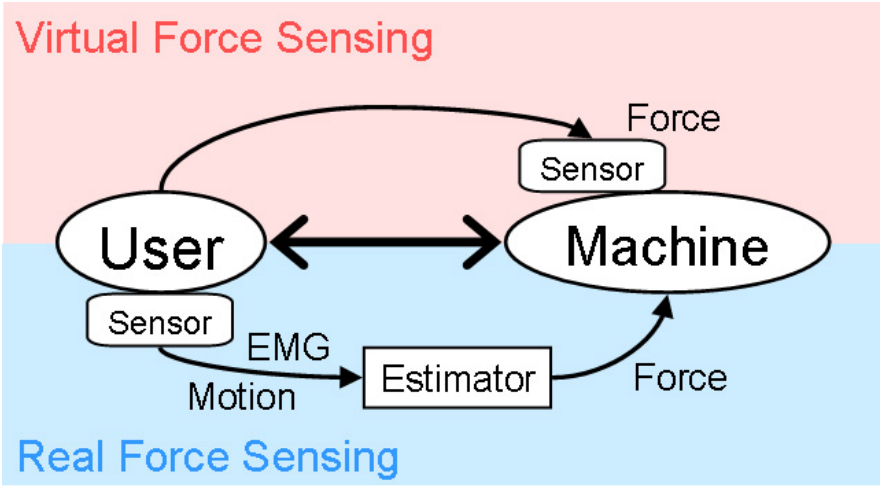

Figure 1. Comparison of force sensing process

by the sensor attache on the user. VFS approach needs the step that train the parameters of the estimator in advance (calibration stage). In the calibration stage, it is needed a force sensor or objects which known mass/inertia to obtained the force applied to the hand, since the force is used for training the parameters of the estimator as a teacher signal.

2.3 Experimental Setup

Figure 2 shows an experimental system to investigate the feasibility of my approach. The system consisted of a robot, a surface electromyograph and an optical motion capture device. The EMG and the markers' positional data were sent to a standard PC for controlling the robot in real time. The motor commands for the robot were

determined based on these sets of data.

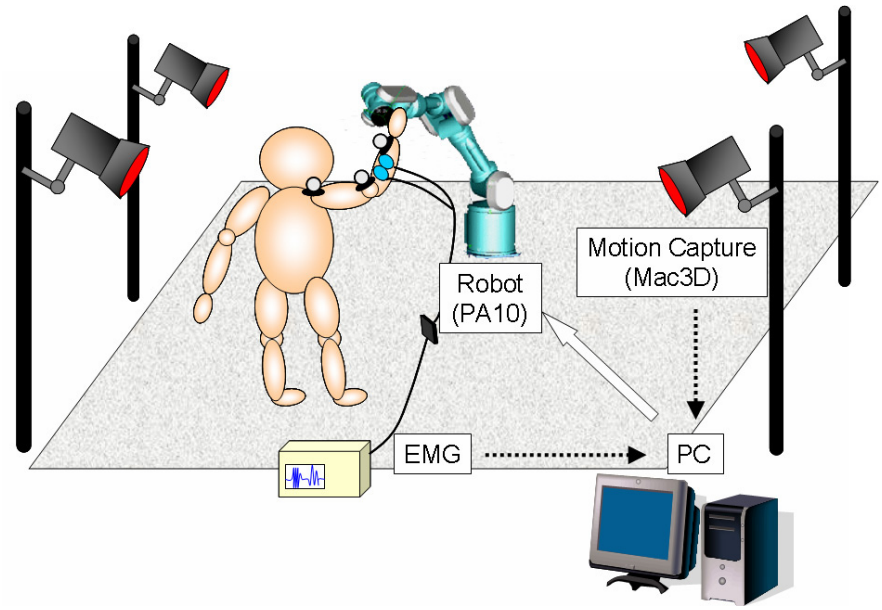

Figure 2. System overview

The detail of system is presented in Figure 3 with diagram. The robot used in the experiment was an industrial six-DOF manipulator, PA10 (Mitsubishi Heavy Industries, Ltd.) which possessed no force/tactile sensors. EMG signals were measured by a compact-electromyograph BA1104 (Digitex Laboratory Co., Ltd.) with active-type electrodes and the telemeter unit TU-4 (Digitex Laboratory Co., Ltd.). The motion capture device was Mac3D system (Motion Analysis Corporation). In the future, it is desired that motion is measured by compact and cheap network camera or acceleration sensor attached on the user. However, because it make the estimation procedure to be complex, I employed motion capture device, though the system becomes big and expensive. EMG signals were digitized by the A/D converter of the Mac3D. The sampling frequency was 200 Hz for both the recording of the EMG signals and the output driving signals. The angular velocity of each joint of PA10 was similarly controlled at a frequency of 200 Hz.

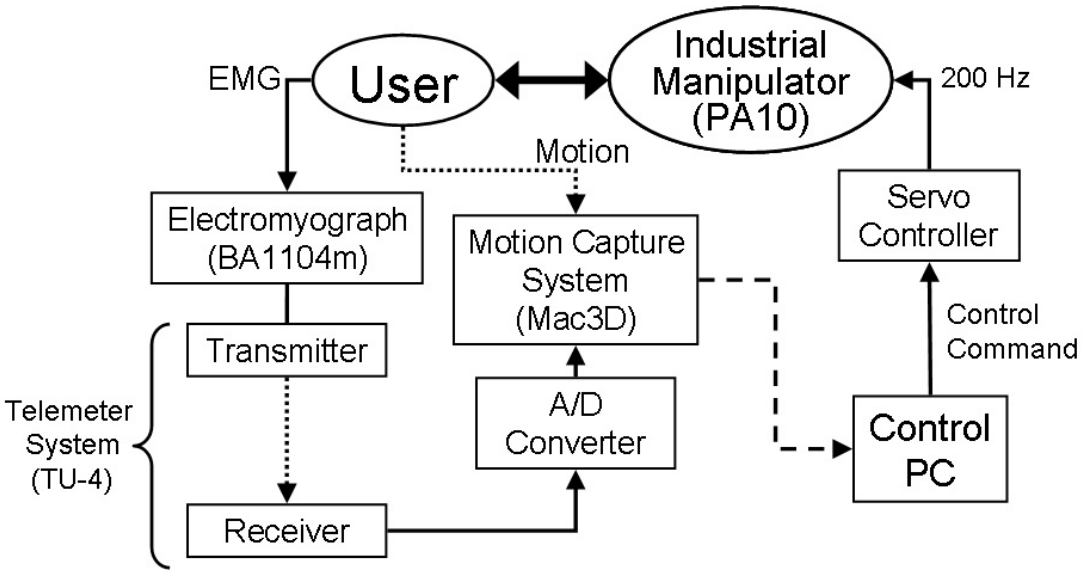

Figure 3. System diagram

3. Kinetic Human-Machine Interaction with the Virtual Sensing Method

To examine the feasibility of my approach, three experiments were conducted. In the first experiment, two joints of the robot were controlled to see whether the robot can obtain force senses by receiving user's biological signals in real-time, and whether the user can make use of the robot's simulated dynamics. The second experiment was conducted to see if the robot can behave as if it had force/tactile sensors over its body. The third experiment was designed to demonstrate that my approach could be useful for making a dynamic and cooperative task take place between a robot and a user.

3.1 Experiment 1: Two-joints control using EMG and the postural information of the hand

The task in this experiment was to control the two joints of the robot (cf. Figure 4) using both EMG and the postural information of the user's hand. The applied force vector was estimated from the amplitude of the estimated force from EMG, and the direction of the force was determined from the hand posture. The task for the robot was to make a movement in the direction of the force applied by a user, and to return to the initial position when the user relaxes its muscle. The applied force vector was

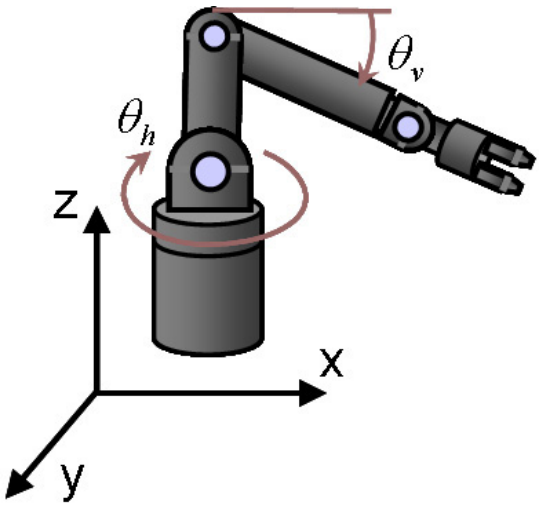

Figure 4. Controlled joints of PA10 in Experiments 1 and 2

determined by the user's force estimated from EMG, and the direction of the force was determined from the user's hand posture. The task for the robot was to make a movement in the direction of the force applied by a user, and to return to the initial position when the user relaxes its muscle.

The muscle subjected to EMG measurement was the flexor carpi radialis (FCR) (Figure 5(a)), and three markers associated with the motion capture device were attached to the back of the user's hand (Figure 5(b)).

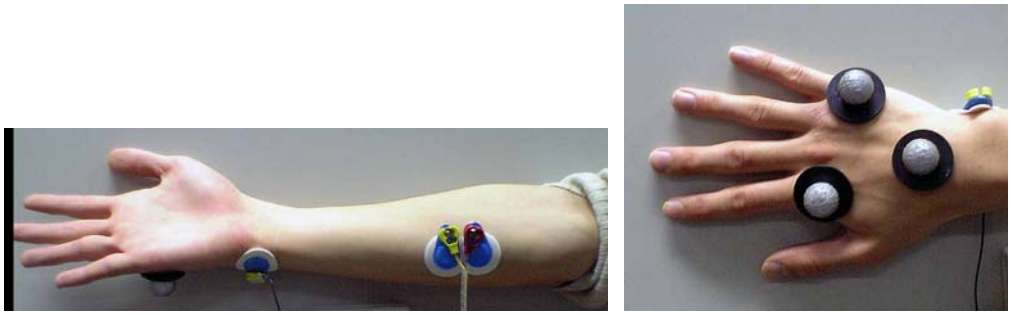

(a) Electrode positions in experiment 1 and 2

(b) Marker positions in Experiment 1 and 2

Figure 5. Electrodes and markers in Experiment 1 and 2

3.1.1 Estimation of the force applied by the hand

First of all, I conducted a pilot experiment in which the EMG and corresponding force data were obtained, and the relationship between them was examined. The force was measured by a force sensor (BL Autotec, Ltd.) with a load rating of 5 $[\mathrm{kgf}]$. The data were taken from the right hand of a subject (a healthy man, 24 years old). The force sensor was fixed on the table, and the table's height was adjusted to touch the subject's forearm when the subject was in a relaxed posture. The subject was instructed to place his palm in the lateral direction and to apply horizontal force to the sensor by wrist flexion. The force and EMG were recorded simultaneously at a sampling frequency of 500 Hz. The acquired EMG data were processed by full-wave rectification, five-point averaging, and low-pass filtering (cutoff frequency of 3.6 Hz) (Figure 6, upper panel).

The lower panel of Figure 6 shows that a linear approximation function is sufficient for describing the relationship, that is:

$$F(t) = C_1 \cdot EMG_{FCR}(t) + C_2 \cdot EMG_{FCR}(t-1) + \cdots + C_{30} \cdot EMG_{FCR}(t-29) + C_{31}, \tag{1}$$

where $F(t)$ and $EMG_{FCR}(t)$ are the estimates of the force applied by the hand and the measured EMG of FCR at a time t, respectively. C_i $(i = 1, 2, \cdots, 31)$ were determined so as to best match the acquired data in terms of minimizing the root-mean-square (RMS) of the sum of the differences of the data fit between the measured data and the linear approximation function. In general, the relationship between EMG and output force shows nonlinearity due to the muscle properties [38]. So I applied a nonlinear function approximation employing a three-layer perceptron [58] to the data, but no significant improvement in data fitting was observed. The reason for this linear relationship is attributed to the fact that the wrist angle of the subject was around 0 degrees at which both the flexor and the extensor muscles of the wrist were relaxed. The upper panel of Figure 6 shows the time-series of the rectified EMG and the filtered EMG. The lower panel of Figure 6 demonstrates the linear mapping from the rectified and filtered EMG to the filtered force data. The RMS error for the test data was 0.458 [N], which was small enough for my study. Though the wrist and arm posture may affect the EMG signal of the FCR, I confirmed that the force amplitude can be accurately estimated from experimental data without considering the wrist and arm posture. This occurs because the wrist angle of the subject was consistently around zero degrees as previously mentioned. Furthermore, the arm posture did not change much. If the posture had changed a lot, adding terms corresponding to additional joints to Equation (1) would deal with the errors due to the changes.

3.1.2 Control law

In this task, angular velocity $\frac{d\theta(t)}{dt}$ was calculated from the force of the user's hand by

$$J\frac{d^2\theta(t)}{dt^2} + c\frac{d\theta(t)}{dt} + k\theta(t) = F(t) \cdot A, \tag{2}$$

where J, c and k were inertia, viscosity and spring. I configured them 0.025 [$\mathrm{kg \cdot m^2}$], 0.50 [$\mathrm{N \cdot m \cdot s}$] and 5.0[$\mathrm{N \cdot m}$], respectively. A is constant that has a dimension of [m].

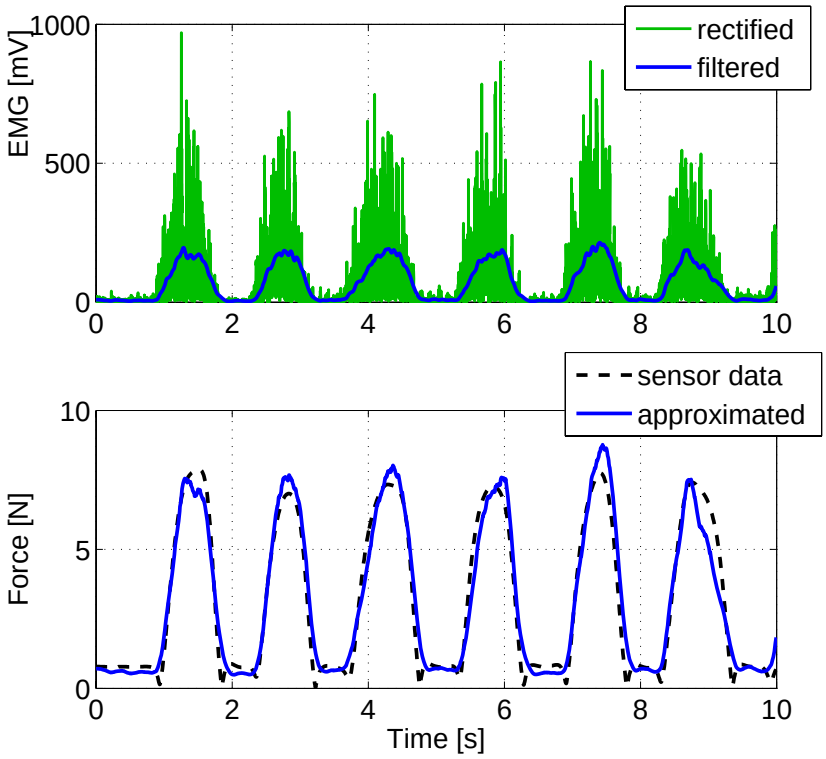

Figure 6. The force estimated from EMG

After that, I divided the desired velocity, $\frac{d\theta(t)}{dt}$, into horizontal and vertical components according to the hand posture as $\phi(t)$:

$$\begin{aligned} \dot{\theta_h} &= \frac{d\theta(t)}{dt}\cos\phi(t) \\ \dot{\theta_v} &= \frac{d\theta(t)}{dt}\sin\phi(t), \end{aligned} \tag{3}$$

where $\dot{\theta_h}$ and $\dot{\theta_v}$ were the joint velocity commands sent to the robot.

Figure 7 shows the definition of the posture of the user's hand. In this figure, the coordinate system (x, y, z) is defined so that the z-y plane is frontal to the user and the x-y plane parallel to the floor. The schematic triangle at the lower right represents the positions of the three markers attached to the back of the user's hand, and the hand posture was represented by ϕ, i.e., the angle of the normal vector of the triangle projected onto the frontal plane from the x-axis coordinate.

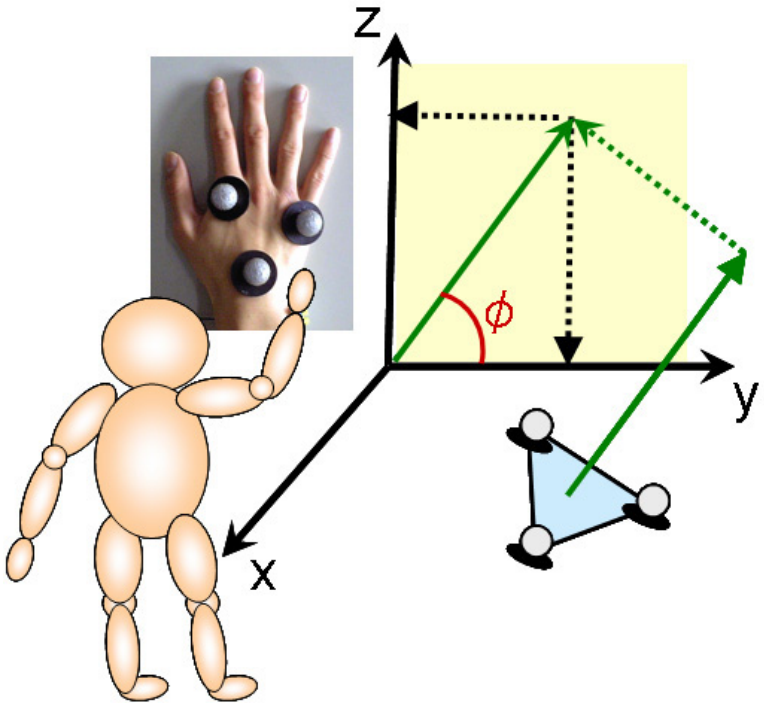

Figure 7. Definition and coordinates of the hand posture

3.1.3 Results

Figure 8 shows some examples of motions during this task. The subjects were instructed to move the robot in the horizontal direction, vertical direction and oblique direction, and then to repeat this sequence of movements. Figure 8 shows the changes of the rectified and the filtered EMG (top panel), the two joint angles (in horizontal and vertical directions) of the robot (middle panel), and the postural information of the hand (bottom panel). These results clearly show that the robot changed its motion

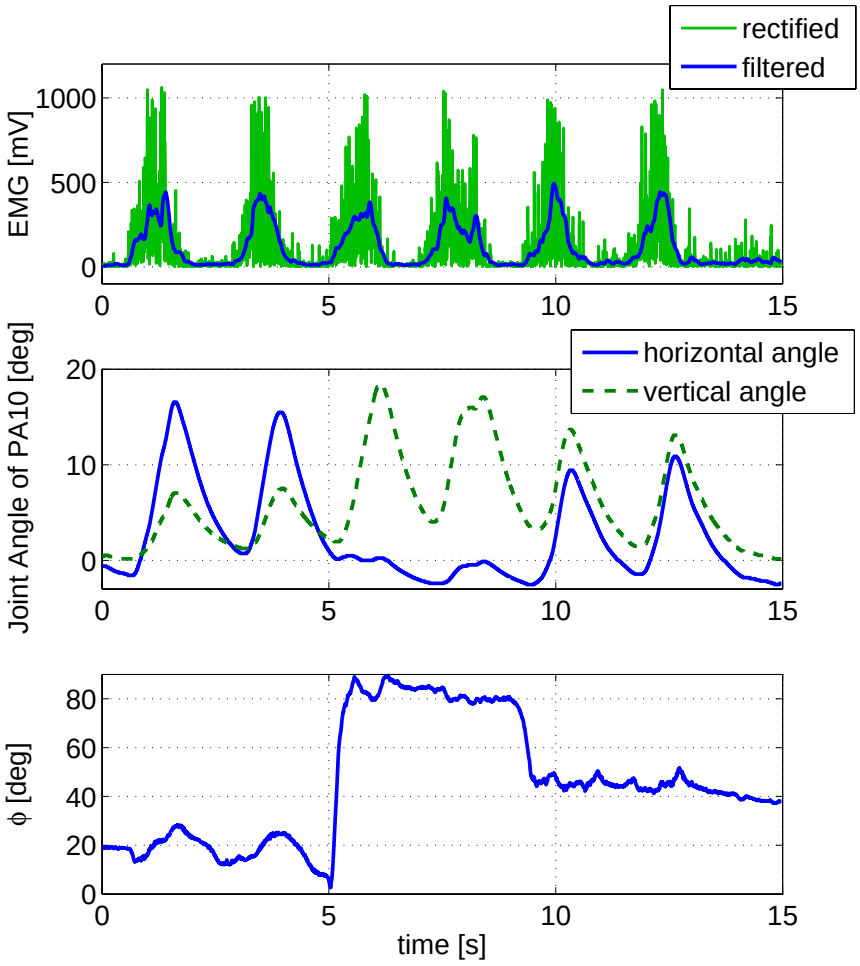

Figure 8. Results of Experiment 1

smoothly according to the amplitude of the subject's force (EMG) and moved in the

direction according to the hand posture, indicating that the robot appropriately sensed the force vector applied by the user.

3.2 Experiment 2: Two-joints control with the power point changing using EMG and the postural information of the hand

This experiment was designed to demonstrate that my system was able to realize distributed force/tactile sensing over the robot's body. The applied force vector was determined by the user's force estimated from EMG, and the direction of the force was determined from the user's hand posture. The procedure of estimating the applied force by the user's hand was the same as that described in 3.1.1. The control law for the two joints of the robot was the same as Experiment 1 except that the robot also modulated its motion according to the power point at which the user applied the force.

I measured EMG from the muscle, flexor carpi radialis (FCR) (cf. Figure 5(a)), and three markers were attached to the back of the user's hand (cf. Figure 5(b)) as in the case of the Experiment 1. Furthermore, two additional markers were attached to the robot (Figure 9) to calculate the length of the manipulator's arm.

3.2.1 Control law

The control law is given by

$$J\frac{d^2\theta(t)}{dt^2} + c\frac{d\theta(t)}{dt} + k\theta(t) = F'(t) \cdot A. \tag{4}$$

The emulated dynamics by the robot were the same as those in the Experiment 1, but the input $F'(t)$ was determined by the following equation:

$$F'(t) = F(t)\frac{l(t)}{l_{\rm arm}}, \tag{5}$$

where $F(t)$ is the force applied by the user's hand, $l_{\rm arm}$ is the length of the robot's arm, and $l(t)$ is a moment arm defined by the distance between the supporting point and the power point estimated from the positional information of the user's hand (Figure 9). In my system, the resolution of $l(t)$ depends on the accuracy of the hand position (power point) measured by my motion capture device, which was found to be as small as 1 [mm].

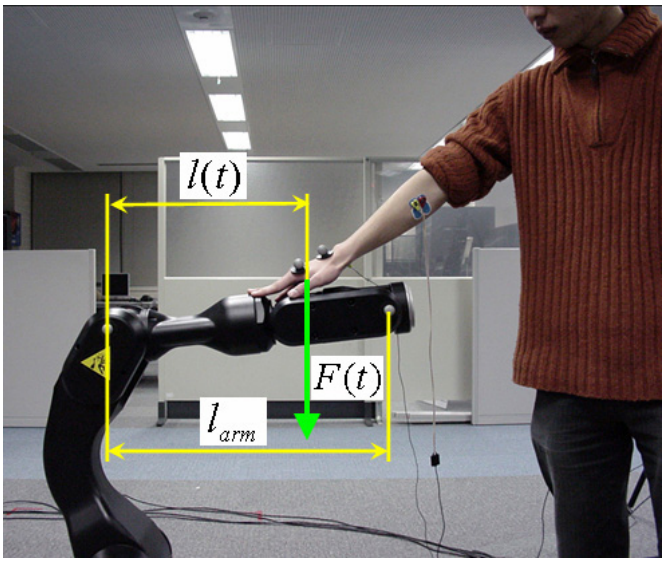

Figure 9. A sample power point and an associated moment arm

3.2.2 Results

Figure 10 shows an example of the results. The subjects were instructed to move the robot arm in the horizontal direction and then in the vertical direction, by changing the power point so that the applied force was kept constant (as far as possible). The figure shows the time course of the rectified and the filtered EMG (top panel), the two joint angles (in the horizontal and vertical directions) of the robot (second panel), the postural information of the hand (third panel), and the power point $l(t)/l_{\rm arm}$ (bottom panel). $l(t)/l_{\rm arm}$ was one when the power point was at the tip of the arm, while it was zero at the root of the arm. These panels indicate that the robot arm changed its motion amplitude according to the power point to which the force was applied, whereas the subject exerted the equivalent force (see EMG data in Figure 10). The results obtained in this experiment demonstrate that the robot successfully behaved as if it had sensed the force vector applied to its body, and changed its behavior according to the changes of the power points. In addition, the subjects reported that the robot was performing as intended, and they felt as if they were pushing a springy bar.

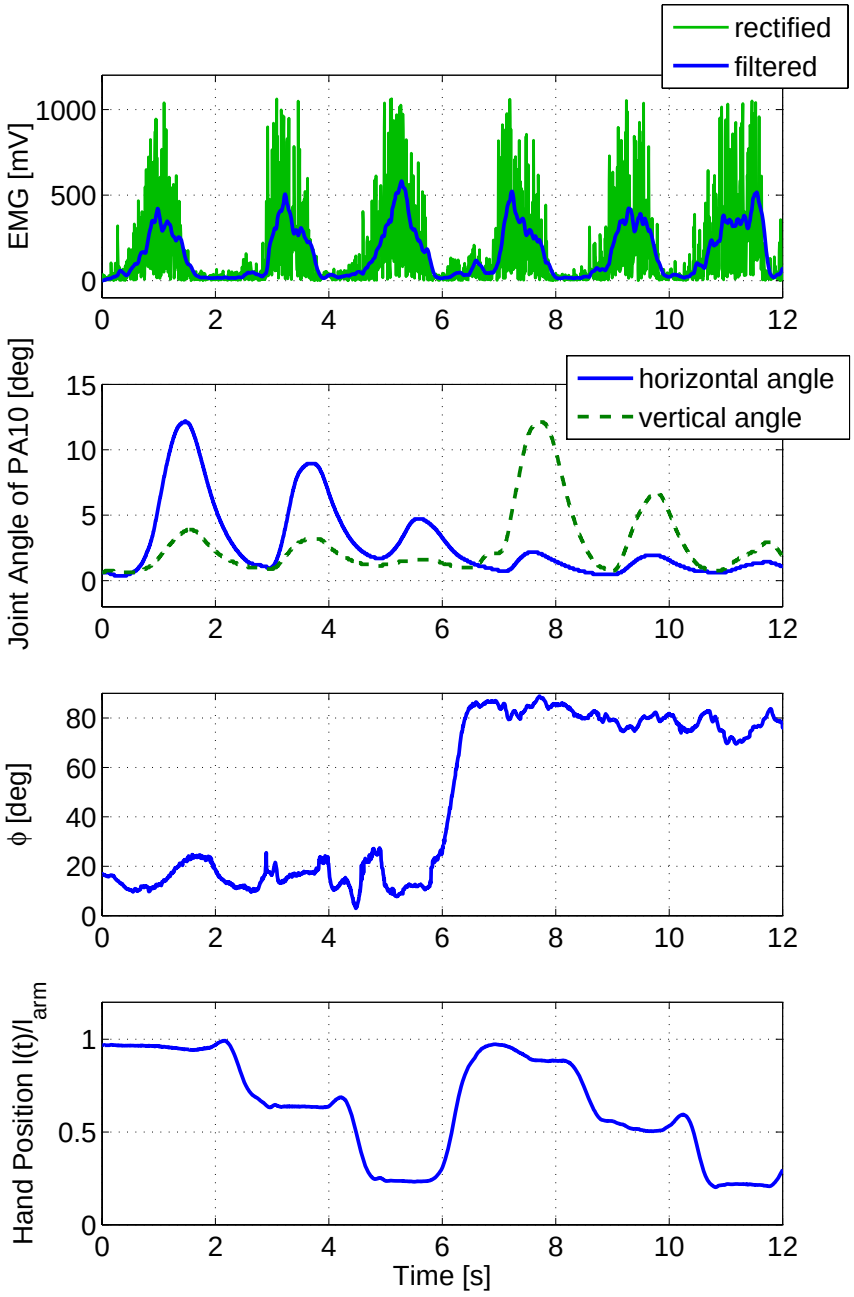

Figure 10. Results of Experiment 2

3.3 Experiment 3: One-dimensional Cooperative holding

Third, I attempted a specific cooperative exercise by this system and a user. In this experiment, the user was requested to move a heavy load up and down along the vertical axis cooperatively with the robot at a defined frequency. Figure 11 is a schematic diagram of this task. The user and the robot exerted the forces f_{u} (target value) and

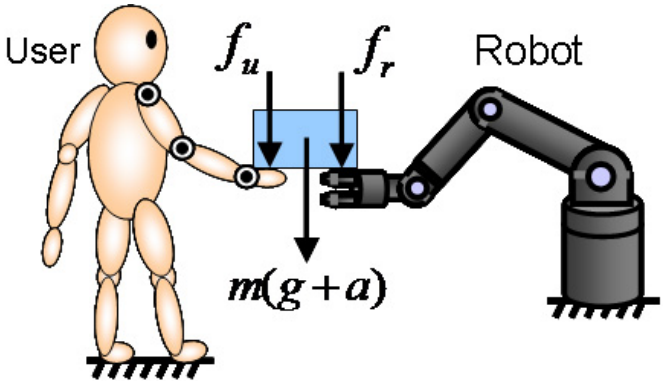

Figure 11. Overview of Experiment 3

f_{r}, respectively, to hold a heavy load of mass m. g and a are the gravity and mass acceleration, respectively. I set $m = 2$ [kg] and f_{u} was assumed to be $\frac{m}{2}(g + a)$. If the force applied to the user's hand was larger than f_{u}, the robot moved upward, while the robot was controlled to move downward when the force was smaller than f_{u}. In this task, the movements of the user and the robot were confined to the sagittal plane, and the user was asked to use only its right upper extremity. The user was also instructed to move the load up and down to specific target points in synchronization with the clicks of a metronome once every 2 [sec]. The target points were set at 0.8, 1.0 and 1.2 $[\mathrm{m}]$ height from the floor. Figure 12 presents examples of the views of this task.

The muscles from which EMG was recorded were the FCR (see section 3.1) and the extensor carpi radialis longus (ECRL) (Figure 13(a)). Five markers for motion capture were attached on the right side of the shoulder, elbow, wrist, and the back of the hand (Figure 13(b)). The joints of PA10 controlled in this experiment were θ_1, θ_2 and θ_3, as shown in Figure 14.

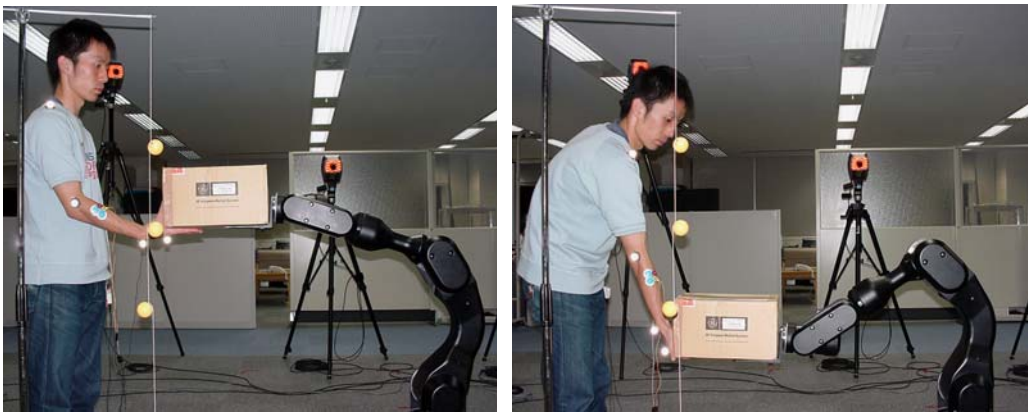

(a) Moving up (b) Moving down

Figure 12. Example views of Experiment 3

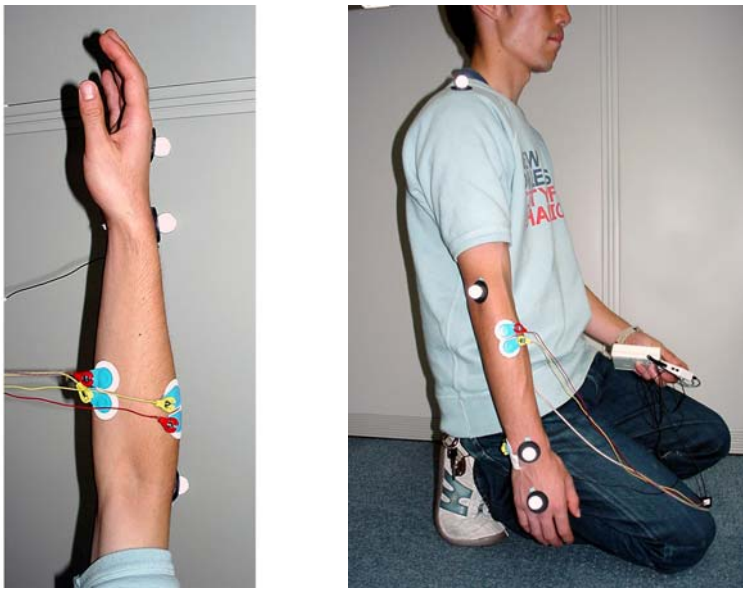

(a) Electrode positions in Experiment 3 (b) Marker positions in Experiment 3

Figure 13. Electrodes and markers in Experiment 3

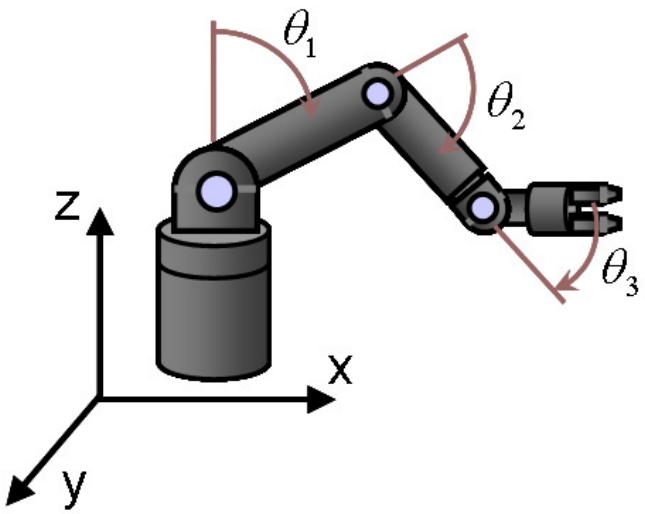

Figure 14. Joints of PA10 controlled in Experiment 3

3.3.1 Estimation of the force bearing on the hand

The force applied to the user's hand, $f_{\mathrm{est}}(t)$, was estimated as follows. (1) the estimation of the wrist torque from EMG signals and motion information, and (2) the calculation of $f_{\mathrm{est}}(t)$ from the dynamic balance between the force and the torque on the tip link (hand), assuming the user's upper extremity to be a three-links manipulator. The benefit of this method is that it uses the estimated torque at the tip joint only, but does not use the torques of the other joints. These processes are described below in detail.

Estimation of the wrist torque The wrist torque τ_{wrist} was estimated from EMG signals, joint angles θ_j, angular velocities $\dot{\theta}_j$ and angular accelerations $\ddot{\theta}_j$ ($j = \mathrm{shoulder}, \mathrm{elbow}, \mathrm{wrist}$). These kinematic values were calculated from the captured motion information by a lin-

ear approximation. The wrist torque was approximated by:

$$\begin{aligned}\tau_{\mathrm{wrist}}(t) =& C_1 \cdot \theta_{\mathrm{shoulder}}(t) + C_2 \cdot \theta_{\mathrm{elbow}}(t) + C_3 \cdot \theta_{\mathrm{wrist}}(t) \\ &+ C_4 \cdot \dot{\theta}_{\mathrm{shoulder}}(t) + C_5 \cdot \dot{\theta}_{\mathrm{elbow}}(t) + C_6 \cdot \dot{\theta}_{\mathrm{wrist}}(t) \\ &+ C_7 \cdot \ddot{\theta}_{\mathrm{shoulder}}(t) + C_8 \cdot \ddot{\theta}_{\mathrm{elbow}}(t) + C_9 \cdot \ddot{\theta}_{\mathrm{wrist}}(t) \\ &+ C_{10} \cdot EMG_{\mathrm{FCR}}(t) + C_{11} \cdot EMG_{\mathrm{ECRL}}(t) \\ &+ C_{12} \cdot EMG_{\mathrm{FCR}}(t-1) + C_{13} \cdot EMG_{\mathrm{ECRL}}(t-1) \\ &+ C_{14} \cdot EMG_{\mathrm{FCR}}(t-2) + C_{15} \cdot EMG_{\mathrm{ECRL}}(t-2) + \cdots \\ &+ C_{48} \cdot EMG_{\mathrm{FCR}}(t-20) + C_{49} \cdot EMG_{\mathrm{ECRL}}(t-20) + C_{50}.\end{aligned} \tag{6}$$

The constants C_i $(i = 1, 2, \cdots, 50)$ were obtained by a polynomial fit to the wrist torques when the subject arbitrarily lifted the weights of 500, 1000, 1500 and 2000 [g] up and down in the calibration stage. The wrist torque was calculated from the motional information by employing inverse dynamics based on the three-links model. EMG_{FCR} and EMG_{ECRL} were normalized by the average of EMG signals acquired when the subject exerted the maximum isometric force. This processing was necessary because the amplitude of EMG often varied with the postural changes of the user and the positions of the attached electrodes. Equation (6) was expected to deal with changes in posture, because it contains the motion information of three joints in the calibration stage. I confirmed that Equation (6) with the parameters obtained in the calibration stage had a generalized power form, through the validation test with the training and test datasets.

Estimation of the force bearing on the hand The dynamic balancing between the force and the torque on every link can be described by the Newton-Euler equation of motion. The torque of tip joints (wrist) was obtained by the procedure above (Equation (6)), and the applied force to the tip link (hand) was calculated by the following procedure. The acceleration of gravity center, angular velocity and angular acceleration of the tip link, which were needed to calculate the force applied to the tip link, were acquired from the motion information. The relationship between the torque at the i-th joint and the moment vector $\boldsymbol{n}_i$ for the i-th link from the $(i-1)$-th link is given by

$$\tau_i = \boldsymbol{q}_i^T \boldsymbol{n}_i + D_i \dot{\theta}_i + E_i(\dot{\theta}_i, \theta_i). \tag{7}$$

$\boldsymbol{q}_i$ is the vector denoting the rotational axis, that is, the y-axis, $\boldsymbol{q}_i = [0\ 1\ 0]^T$. D_i and $E_i(\dot{\theta}_i, \theta_i)$ are the viscous friction coefficients for the joint and the nonlinear friction torque, respectively, and they were set at 0 for simplicity. The dynamic balancing between the force and the moment about the i-th link is described by the Newton-Euler equation of motion:

$$\boldsymbol{n}_i = \boldsymbol{A}_{i+1}\boldsymbol{n}_{i+1} + \boldsymbol{I}_i\dot{\boldsymbol{\omega}}_i + \boldsymbol{\omega}_i \times (\boldsymbol{I}_i\boldsymbol{\omega}_i) + \boldsymbol{a}_i \times (m_i\ddot{\boldsymbol{p}}_{gi}) + \boldsymbol{l}_i \times \boldsymbol{A}_{i+1}\boldsymbol{f}_{i+1}. \quad (8)$$

$\boldsymbol{A}_i$, $\boldsymbol{I}_i$, $\boldsymbol{\omega}_i$, $\boldsymbol{a}_i$, m_i, $\boldsymbol{p}_{gi}$, $\boldsymbol{l}_i$, and $\boldsymbol{f}_i$ are a coordinate transformation matrix from the $(i-1)$-th to the i-th coordinate systems, an inertia matrix on the gravity center of the i-th link, an angular velocity vector of the i-th link, a vector from the origin to the gravity center of the ith link, a mass of the i-th link, a vector from the world origin to the gravity center of the tip link, a vector from the origin of the i-th link to the origin of the $(i+1)$-th link, and a force vector which acts on the i-th link from the $(i-1)$-th link, respectively. Making use of Equations (7) and (8), the force applied to the user's hand, $f_{\mathrm{est}}(t)$, can be estimated by

$$f_{\mathrm{est}}(t) = \frac{\tau_{\mathrm{wrist}} - I_{3y}\dot{\omega}_{3y} - a_3 l_3 \ddot{p}_{3gx}}{l_3 \sin(-\theta_1 - \theta_2 - \theta_3)}, \quad (9)$$

where I_{3y}, ω_{3y}, p_{3gx}, m_3, l_3 and a_3 are the y-component of the tip link inertia, the angular velocity of the tip link, the x-component of the vector from the world origin to the gravity center of the tip link, the mass of the tip link, the length of the tip link, and the distance between the gravity center and the origin of the tip link, respectively. The mass of each link of a human can be estimated from the body height and weight [73].

3.3.2 Control law

The dynamics of the robot hand in the z-direction is given by

$$m\ddot{z}(t) + c\dot{z}(t) + kz = A(f_{\mathrm{est}}(t) - f_{\mathrm{u}}), \quad (10)$$

where m, c, k and A are the mass, viscosity, spring of the robot hand and the amplification constant, respectively. I configured these four parameters at 0.2 [kg], 1.0 [N $\cdot$ s/m], 0.1 [N/m], and 2.0, respectively. The velocity of the robot hand in the z-direction, $\dot{z}(t)$, was determined by the difference between the force exerted by the subject, f_{u}, and the

force applied to the subject's hand, $f_{\mathrm{est}}(t)$. The velocity of the robot hand in the x-direction was controlled so that $\dot{x}(t)$ was maintained at 0. The angular velocities sent to PA10, $\dot{\theta_1}$ and $\dot{\theta_2}$, were calculated by

$$\begin{bmatrix} \dot{\theta_1} \\ \dot{\theta_2} \end{bmatrix} = \boldsymbol{J}(\boldsymbol{\theta})^{-1} \begin{bmatrix} \dot{x} \\ \dot{z} \end{bmatrix}, \tag{11}$$

and θ_3 was obtained by

$$\theta_3 = -\theta_1 - \theta_2, \tag{12}$$

so that the robot hand is maintained in the horizontal position.

3.3.3 Results

Figure 15 represents an example of the motion of this task. The top panel shows the changes of the estimated force applied to the subject's hand, $f_{\mathrm{est}}(t)$, and the second panel shows the changes of the joint angles of PA10. In the bottom panel, the trajectory of the load's height was plotted with the target points indicated by circles. The results indicate that when the subject reduced the force to move the load down, ($f_{\mathrm{est}}(t)$ was smaller than f_{u}), θ_2 was increased and the robot hand moved downward. Conversely, when the subject applied an additional force to raise the load ($f_{\mathrm{est}}(t)$ was larger than f_{u}), θ_2 was decreased and the robot hand moved upward. θ_1 and θ_3 moved in collaboration with θ_2 to keep the posture of the robot hand horizontal. The trajectory of the load successfully tracked the target points, suggesting the feasibility of my approach for dynamic man-machine cooperation.

3.4 Experiment4: Three-dimensional cooperative holding

In this study, I first describe my extension of the work conducted by Tamei, et al. [63] in which the one-dimensional cooperative holding task was achieved by the VFS. In this task, the user is requested to vertically move a heavy load using its an upper limb cooperatively with the robot moving the load vertically, armed with a one-dimensional virtual sensing force operating perpendicular to the back of the user's hand. They demonstrated that the vertical trajectory of the load successfully tracked the pre-defined target points as the user intended, suggesting the feasibility of the VFS approach to kinetic man-machine cooperation.

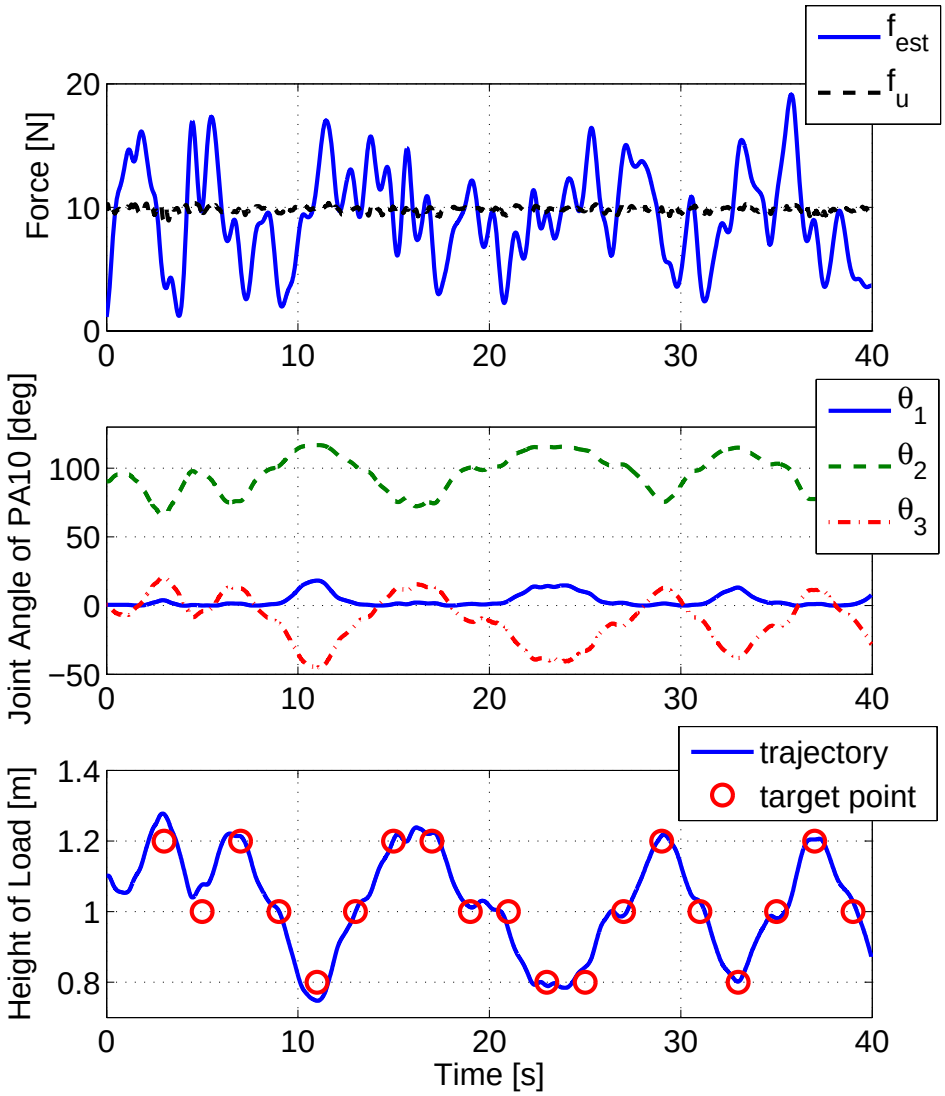

Figure 15. Results of Experiment 3

In this study, I developed a three-dimensional version of the cooperative holding task in which the user was asked to use only the right upper extremity of its arm. Figure 16 provides an overview of this task.

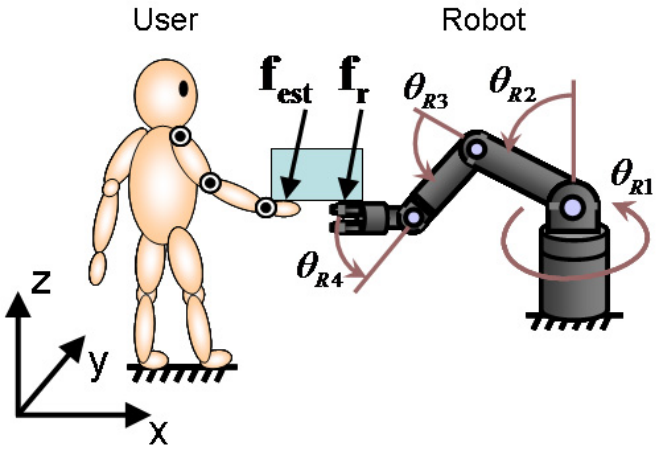

Figure 16. Overview of the Experiment 4

3.4.1 Estimation of the force bearing on the hand based on forward dynamics

For this task, I expanded the force-vector estimator discribed in 3.3.1 to three-dimensional version. The three-dimensional force applied to the user's hand, $\boldsymbol{f}_{\mathrm{est}}(t) \in \boldsymbol{R}^{3\times 1}$ was estimated as following as in the case of the one-dimension; (1) estimation of the each joint torque $\boldsymbol{\tau}_j(t) \in \boldsymbol{R}^{5\times 1}$ from EMG signals and motion information, and (2) calculation of $\boldsymbol{f}_{\mathrm{est}}(t)$ from each joint torque (forward dynamics) using Newton-Euler dynamic equation by assuming the user's upper extremity to be a three-link and 5 DOF manipulator in which joint DOF are three-dimensional rotation of shoulder, one-dimensional rotation of both elbow and wrist. Each joint torque were linearly estimated as

$$\boldsymbol{\tau(t)} = \boldsymbol{W}^T[\boldsymbol{\theta}(t)^T, \dot{\boldsymbol{\theta}}(t)^T, \ddot{\boldsymbol{\theta}}(t)^T, \boldsymbol{m}(t)^T, \boldsymbol{m}(t-1)^T, \cdots, \boldsymbol{m}(t-29)^T, \mathbf{1}^T]^T, \quad (13)$$

where $\boldsymbol{m}(t) \in \boldsymbol{R}^{8\times 1}$ is the EMG signals that were preprocessed by full-wave rectification and low-pass filtering (cutoff frequency of 3.6 Hz), $\boldsymbol{\theta} \in \boldsymbol{R}^{5\times 1}$ is the subject's joint angle vector consisting of three-dimensional rotation of shoulder, on-dimensional rotation of both an elbow and a wrist. The joint angle vectors were calculated from the captured motion information. Parameters in $\boldsymbol{W} \in \boldsymbol{R}^{256\times 5}$ were obtained by fitting to

the data acquired when the subject moved the load cooperatively with the robot using a force sensor in the calibration stage. I used EMG signals with 30 tapped-delay lines corresponding to the period of 150 ms so that a suitable filter for each task would be acquired. The reason for this approach is that it is known that there is a delay between an EMG signal input and the corresponding muscle contraction, and that the delay time varies with the muscle shortening velocity [12, 14, 41].

In the calibration stage, the force was measured by a force sensor and was used to control the robot. In one trial, the force and motion were recorded for 40 seconds, and 10 trials of data were collected in total. Equation (13) was expected to deal with changes in posture, because it contains the motion information of three joints in the calibration stage. Figure 17 shows the performance for the test data. Root-mean-square (RMS) errors were 0.996, 0.983, 0.826, 0.756 and 0.329 $[\mathrm{Nm}]$, respectively, and error rate was less than 5 % in each joint torque. I confirmed that the trained linear estimator (Equation (13)) with the parameters obtained in the calibration stage was a good fit to the data, which was a part of the collected data obtained for the validation test which included the training and test datasets. Since shoulder joint have three-dimensional roatation, it makes the forward dynamics calculation to be more complex than one-dimensional version. More ditails of forward dynamic calculation are described in Appendix A. However, because this dynamics model has very high-sensitivity to the input torque, force estimation based on forward dynamics was suspended.

3.4.2 Estimation of the force bearing on the hand using function approximation

Because the estimation of the force bearing on the hand based on forward dynamics had difficulty discribed above, I reformulated the force estimation as the functional approximation problem. The applied force to the user's hand, $\boldsymbol{f}_{\mathrm{est}}(t)$ was linearly estimated as

$$\boldsymbol{f}_{\mathrm{est}}(t) = \boldsymbol{W}^T[\boldsymbol{\theta}(t)^T, \dot{\boldsymbol{\theta}}(t)^T, \ddot{\boldsymbol{\theta}}(t)^T, \boldsymbol{m}(t)^T, \boldsymbol{m}(t-1)^T, \cdots, \boldsymbol{m}(t-29)^T, \boldsymbol{1}^T]^T, \quad (14)$$

where $\boldsymbol{m}(t) \in \boldsymbol{R}^{8\times 1}$ is the EMG signals that were preprocessed by full-wave rectification and low-pass filtering (cutoff frequency of 3.6 Hz), $\boldsymbol{\theta} \in \boldsymbol{R}^{5\times 1}$ is the subject's joint angle vector consisting of a three-dimensional rotation of shoulder, and a one-dimensional rotation of both an elbow and a wrist. The joint angle vectors were

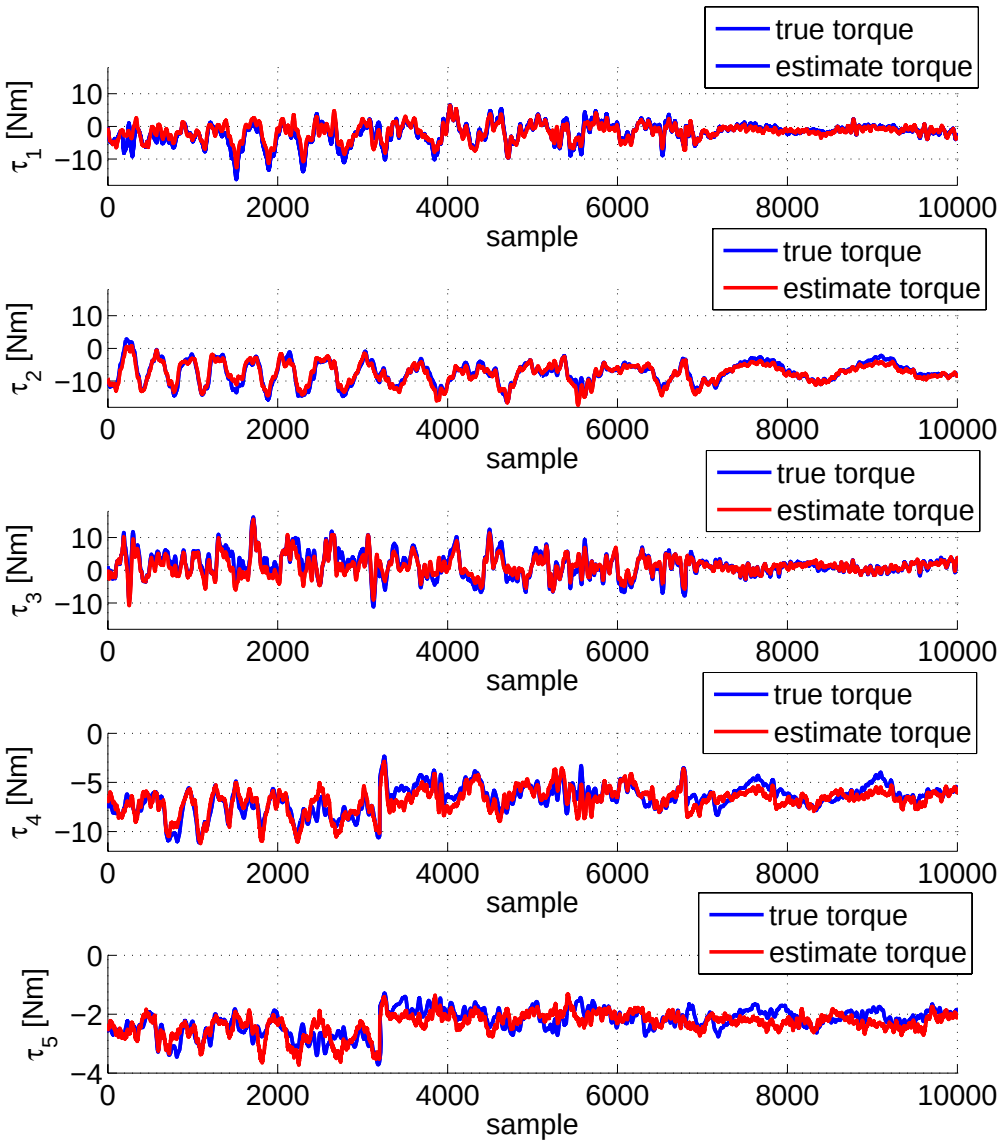

Figure 17. Validation of the linear torque estimator

calculated from the captured motion information. Parameters in $\boldsymbol{W} \in \boldsymbol{R}^{256\times 3}$ were obtained by fitting the same data in 3.4.1.

Equation (14) was expected to deal with changes in posture, because it contains the motion information of three joints in the calibration stage. I confirmed that the trained linear estimator (Equation (14)) with the parameters obtained in the calibration stage was well-generalized for the data, which was a part of the collected data, through the validation test with the training and test datasets. Figure 20 shows the performance for the test data. Root-mean-square (RMS) errors in each direction were 0.699, 0.561 and 0.750 [N], respectively.

3.4.3 Control law

The control dynamics of the robot hand in the each-direction is given by:

$$M_{\mathrm{R}}\ddot{\boldsymbol{p}}_{\mathrm{R}}(t) + C_{\mathrm{R}}\dot{\boldsymbol{p}}_{\mathrm{R}}(t) + K_{\mathrm{R}}\boldsymbol{p}_{\mathrm{R}} = A(\boldsymbol{f}_{\mathrm{inp}}(t) - \boldsymbol{f}_{\mathrm{u}}), \tag{15}$$

where M_{R}, C_{R}, K_{R} and A are the mass, viscosity, spring properties set to the robot hand and the amplification constant, respectively. I set these four parameters to 0.2 [kg], 1.0 [N $\cdot$ s/m], 0.1 [N/m], and 2.0, respectively. $\boldsymbol{p}_{\mathrm{R}} = [x_{\mathrm{R}}\ y_{\mathrm{R}}\ z_{\mathrm{R}}]^T$ is the Cartesian coordinates of the robot hand. The desired velocity of the robot hand $\hat{\dot{\boldsymbol{p}}}_{\mathrm{R}}$ was determined by the difference between the target value of the force applied to the subject's hand, $\boldsymbol{f}_{\mathrm{u}}$, and the force input to the controller, $\boldsymbol{f}_{\mathrm{inp}}(t)$. I assumed $\boldsymbol{f}_{\mathrm{u}} = [0\ 0\ -\frac{M}{2}(g+\ddot{z})]^T$ and set $M = 2$ kg. g and z are the gravity acceleration and the z-coordinate of the load, respectively. The angular velocities, $\hat{\dot{\theta}}_{\mathrm{R1}}$, $\hat{\dot{\theta}}_{\mathrm{R2}}$ and $\hat{\dot{\theta}}_{\mathrm{R3}}$, sent to the robot for control, were calculated as

$$\begin{bmatrix} \hat{\dot{\theta}}_{\mathrm{R1}} \\ \hat{\dot{\theta}}_{\mathrm{R2}} \\ \hat{\dot{\theta}}_{\mathrm{R3}} \end{bmatrix} = \boldsymbol{J}(\boldsymbol{\theta}_{\mathbf{R}})^{-1} \begin{bmatrix} \hat{\dot{x}}_{\mathrm{R}} \\ \hat{\dot{y}}_{\mathrm{R}} \\ \hat{\dot{z}}_{\mathrm{R}} \end{bmatrix}, \tag{16}$$

and $\hat{\theta}_{\mathrm{R4}}$ was obtained by:

$$\hat{\theta}_{\mathrm{R4}} = -\hat{\theta}_{\mathrm{R2}} - \hat{\theta}_{\mathrm{R3}}, \tag{17}$$

so that the robot hand was kept horizontal.

Figure 2 shows an overview of an experimental system to investigate the feasibility of my approach. The system was consisted of a robot, a surface electromyograph and an optical motion capture device. The EMG and the markers' positional information

Figure 18. Example view in the Experiment 4

were sent to a standard PC for controlling the robot in real time. The motor commands for the robot were determined based on these sets of information.

Figure 18 presents a view in the experiment. The muscles for which EMG was recorded were Deltoid-clavicular part (DELC), Deltoid-acromial part (DELA), Deltoid-scapular part (DELS), Biceps brachii long head (BB), Pectralis major Clavicular head (PM), Triceps brachii lateral head (TB), Flexor carpi radialis (FCR) and Extensor carpi radialis longus (ECRL) (Figure 19(a)). Six markers for motion capture were attached to the left shoulder, the right side of the shoulder, the elbow, the wrist, and the back of the hand (Figure 19(b)). The controlled joints of PA10 were θ_{R1}, θ_{R2}, θ_{R3} and θ_{R4}, as shown in Figure 16.

3.4.4 Results and problems

Figure 21 presents an example of results in which the experiment was conducted for $\boldsymbol{f}_{\mathrm{inp}}(t) = \boldsymbol{f}_{\mathrm{est}}(t)$. The top panel shows the changes of the estimated force applied to the subject's hand, $\boldsymbol{f}_{\mathrm{est}}(t)$. The second to the bottom panel shows the trajectory of the load in each direction, with the target points indicated by circles. These figures show that the load could not be moved to the target points successfully even though the virtual force estimation was good enough for the test dataset in the calibration

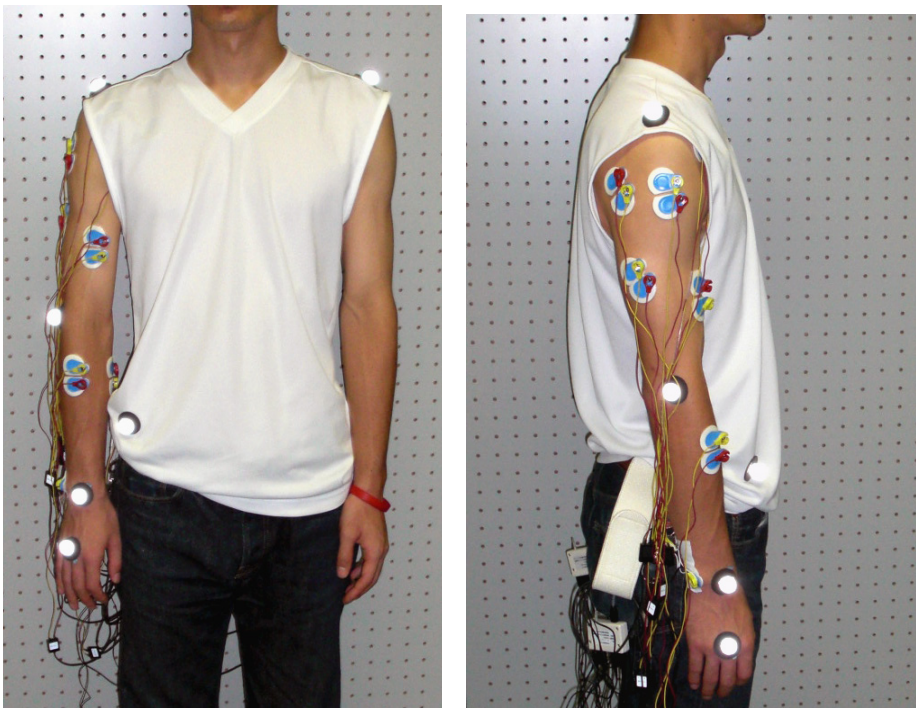

(a) Front view (b) Side view

Figure 19. Electrodes and markers in the Experiment 4

procedure, as shown in Figure 20.

3.5 Discussion

I have proposed a new approach to designing intelligent machines that can work for humans not only in industrial factories but also in our daily life such as at home. The key to the approach is the virtual realization of force/tactile sensors in robots by using user's biological signals such as EMG and postural information. In the experiments, I demonstrated that an industrial robot manipulator possessing no force/tactile sensors successfully achieved dynamic and even cooperative interactions with humans. In the first two experiments, the impedance control was performed on the two joints of the robot arm. The input to the impedance controller was the force vector estimated by an-

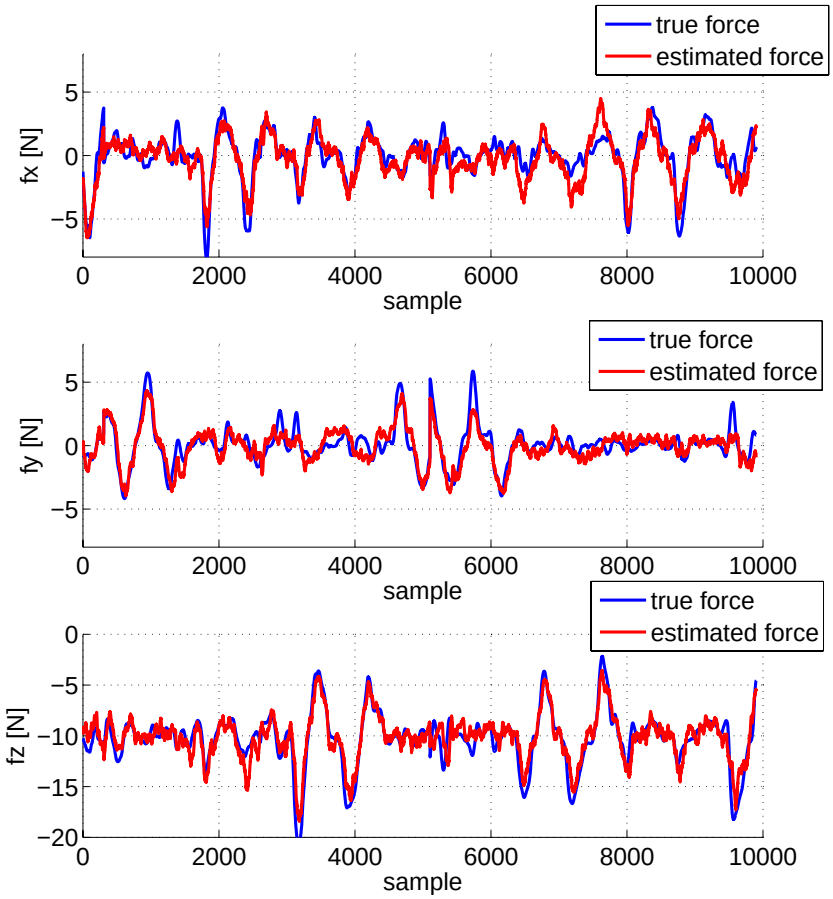

Figure 20. Validation of the linear estimator

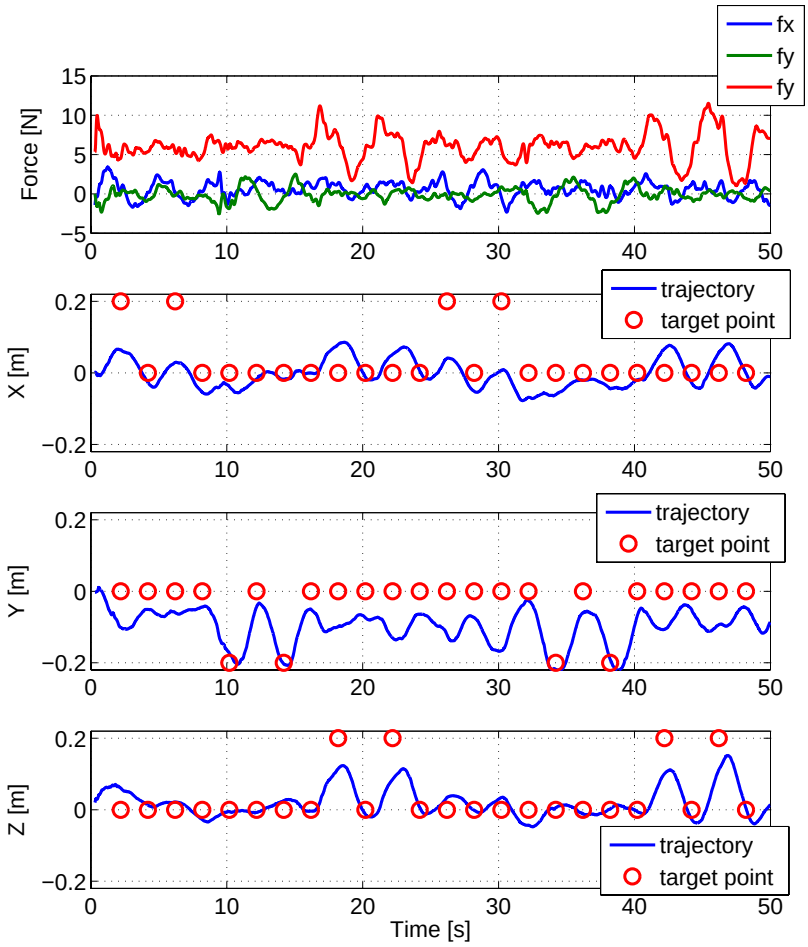

Figure 21. Results of Experiment 4

alyzing the subjects' biological signals. The observed behaviors acquired by the robot as well as the results of questionnaires to the subjects assured us that the subjects intuitively and easily performed the task, suggesting that my approach could be applicable to haptic devices. In Experiment 1 and 2, additional calibration processes to update the parameters of Equation (1) were not critically necessary after the electrodes were replaced or the subjects were changed, although the additional calibration process would increase the accuracy of the force estimation. In the third experiment, as a realistic cooperative exercise, the task of cooperatively holding and moving a heavy load was conducted and successful results were obtained. The force applied to the hand was obtained from the dynamic balance between the torque and the force of the tip link as shown in Equation (9). This method has such an advantage that it requires the torque estimation only for the tip joint even in the case of multijoint movement, and then the number of muscles to measure EMG signals can be small. Therefore, allowing the user to generate more complicated motion with more joints will be feasible. However, it was difficult to realize fast and accurate moves of the load. To achieve faster movements, I am planning to improve the virtual force sensor by incorporating more muscles as well as a variety of user's behaviors, which would require a more powerful function approximation method. A recalibration stage was necessary when a subject was changed in this experiment. Implicit, easy and automatic calibration is desirable, which could be achieved, for example, by just recording user's behaviors including interactions with objects in ubiquitous computing environments in which mass/inertia of many objects are known.

Although my current system is relatively large and difficult to carry, this will not be a big problem in the near future, since networked-cameras and computers are becoming ubiquitous (e.g., [50, 31]), and EMG measurement devices are becoming portable. Alternatively, it will be possible to estimate the postures and motions of a user only from EMG signals (e.g., [35, 67]). It will also be possible to estimate the user's posture by combining information from a camera and a cheap inertial sensor [64], or cheap inertial and magnetic sensors attached to the subject without external sensors such as camera [3, 24]. I could also imagine employing glove-like devices which measure hand forces, postures [46] and EMG simultaneously. The data of position and posture obtained by cheap sensors may lose some accuracy, but it is expected that good accuracy is achieved by data fusion(e.g., [64]). Even so, there might be a difficulty in obtaining

the accurate acceleration which requires double differentiation of the position information. Though the angular acceleration of each joint based on motion-captured data was used for the estimation of wrist torque as shown by Equation (6), I could omit terms using angular accelerations because I made sure that their contributions to the estimation is very small (less than 0.0025 %), which can relax the requirement for acceleration sensing. When calculating the force applied to the hand in Equation (9), acceleration of the gravity center of the tip link, $\ddot{p}_{3gx}$, was necessary, but it can be easily measured by a cheap inertial sensor. If the number of sensors to be attached to the user in an unorganized manner increases, the user would feel uncomfortable. Glove-like devices in which cheap inertial and positional sensors and electrodes for EMG are attached in an organized manner could solve the above issue. It is notable that my approach is not confined to what I call "robots", but rather it should be useful for various intelligent machines as mentioned in Section 2.2.

My future work will take more muscles and more sensor devices into account for more precise and robust force estimation. I am also interested in the estimation of various internal states of humans, such as the impedance of arms and the ultimate intentions of the humans, which could be helpful for cooperating tasks [29, 17]. My long-term goal is to achieve full-body cooperation between a humanoid robot and its user based on the measurement of the full-body muscles of the users, and possibly of internal states like the intentions of users.

4. Reinforcement Learning for Kinetic Human-Robot Co-operation

In 3.4, I presented ne of the applications of the virtual force sensing approach to the three-dimensional cooperative holding task, and then pointed out an inherent difficulty in the use of EMG signals caused by the fact that the muscle coordination can vary over time. To overcome this difficulty, I proposed an application of reinforcement learning [61] to the VFS. There are previous papers that relate the interaction of a user and a robot using reinforcement learning [65, 48], however, papers that is dealing with physical interaction are less common. The example of applications to the cooperative holding task demonstrate the feasibility of my approach.

4.1 Overview of reinforcement learning of the cooperative holding task

As discussed before, my desire was to achieve an accurate three-dimensional cooperative holding task. I introduce reinforcement learning beause it enable the robot controller to be adaptive to the changes of EMG pattern and the muscle coordination in an on-line without explicit teacher signals. Because no explicit teacher signals could be given, I reformulated this problem as a reinforcement learning problem. The overview of reinforcement learning of the task is illustrated in Figure 22. The goal of policy optimization in reinforcement learning is to optimize the policy parameters so that the expected reward becomes maximal. In my approach, there are two conditions on applying reinforcement learning to approximate the whole process as a Markov decision process (MDP) [5]. First, a computer agent and the user should share the same goal represented by a reward function. Second, the environment should include the user because not only the robot's state but also the user's state should be observed as much as possible.

4.2 Formulation

The implimentation overview of reinforcement learning for the task is shown in Figure 23. The computer agent observes the user's EMG and motion signals, and optimizes the policy $\boldsymbol{a}$ as the additional term to the estimated force. That is, the force input

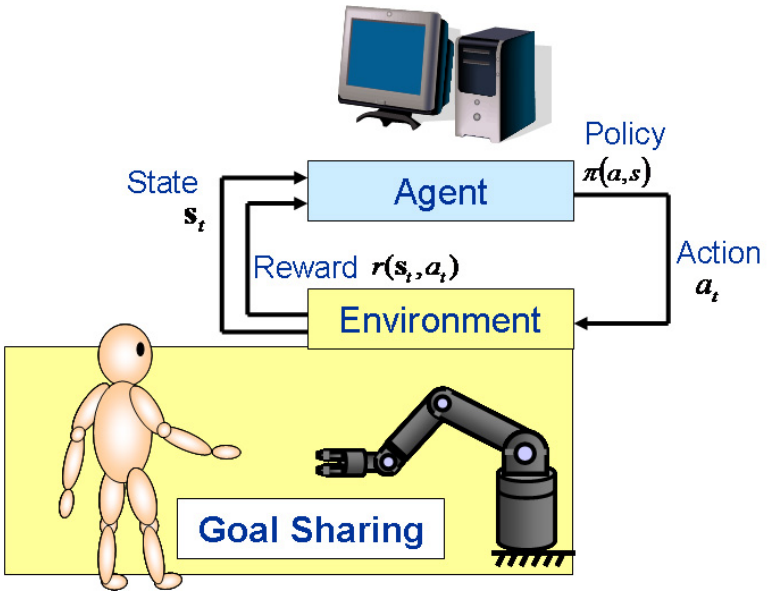

Figure 22. Scheme of reinforcement learning

to the controller (Eq. (15)) is calculated by:

$$\boldsymbol{f}_{\text{inp}} = \boldsymbol{f}_{\text{est}} + \boldsymbol{a}. \tag{18}$$

As stated in Section 4.1, the user and the robot should share the same goal. For this condition, the task design was rearranged as a reaching task, i.e., the user and the robot were requested to move a load cooperatively to a specified location in specified time. In other words, the spatiotemporal specification was the shared goal.

I employed the on-line version of the GARB algorithm [68] for reinforcement learning. The on-line GARB is a policy-gradient method which is suitable for the robot learning problem, cf., Appendix. The advantages of the policy gradient method are that the policy representation can be chosen so that it is meaningful for the task and can incorporate domain knowledge. This often requires fewer parameters in the learning process than in value-function based methods. In addition, the policy gradient method can be used model-free.

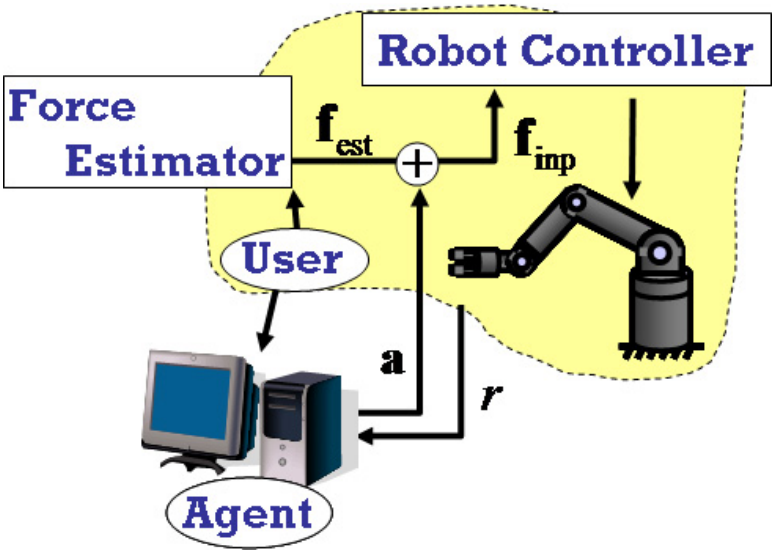

Figure 23. Implementation of the policy gradient learning

4.3 Experiment1: learning based on force estimation using a delay-line EMG

The detailed setting for learning is as follows. The state $\boldsymbol{s} \in \boldsymbol{R}^8$, policy $\boldsymbol{a} \in \boldsymbol{R}^3$ and reward $r \in \boldsymbol{R}$ were defined as

$$\boldsymbol{s} \equiv (\boldsymbol{m}, \boldsymbol{p}_{\mathbf{R}}, \boldsymbol{\theta}_{\mathbf{R}}), \tag{19}$$

$$a_i \sim \pi(a_i|\boldsymbol{s}, \boldsymbol{w}_i) = \mathcal{N}(a_i|\mu_i, \sigma_i), \tag{20}$$

$$\mu_i = \sum_j^{N_{\mathrm{EMG}}} w_{ij} m_j,$$

$$\sigma_i = \frac{1}{1 + \exp(-w_{i9})}, \quad (i = x, y, z),$$

$$r = \frac{1}{(2\pi)^2 |\boldsymbol{\Sigma}|^{1/2}} \exp\left\{-\frac{1}{2}(\boldsymbol{x} - \boldsymbol{d})^T \boldsymbol{\Sigma}^{-1} (\boldsymbol{x} - \boldsymbol{d})\right\} \tag{21}$$

$$-\gamma_{\mathrm{A}} \sum_k^{N_{\theta_{\mathrm{R}}}} \exp(-\ddot{\theta}_{\mathrm{R}k}{}^2) - \gamma_{\mathrm{EMG}} \sum_j^{N_{\mathrm{EMG}}} m_j,$$

where $\boldsymbol{m}, \boldsymbol{p}_{\mathbf{R}}$, and $\boldsymbol{\theta}_{\mathbf{R}}$ are the same variables described in the last section, and $\boldsymbol{w}_i \in \boldsymbol{R}^{N_{\mathrm{EMG}}}$ is the parameter vector which was learned by reinforcement learning. The plolicy is given based on gaussian distribution and is equivalent to the adjustment of the

part of parameters of the estimator (14) in on-line. $N_{\theta_{\mathrm{R}}}(=4)$ and $N_{\mathrm{EMG}}(=8)$ are the number of controlled joints of the robot and the measured EMG signals, respectively. The reward function consists of three terms; the first term represents the reaching accuracy in time and space, the second term for smoothness in robot motion, and the third term for energy efficiency. The first term was a normal probability density function in which $\boldsymbol{d} \in \boldsymbol{R}^4$ is the desired load state specified in time t_{target} [s] and the target position in the world coordinates (x_{target}, y_{target} and z_{target} [m]). $\boldsymbol{x}$ is the current load state. $\boldsymbol{\Sigma}$ is a diagonal matrix whose elements were set to 0.2 and 0.002. m_j is the EMG signal of j-th muscle. γ_{A} and γ_{EMG} are constants balancing the contribution of the three terms, and both were empirically set to 0.1.

The reason why I used only the current EMG signals $\boldsymbol{m}(t)$ at the time t among 30 tapped-delay lines for the agent's state $\boldsymbol{s}(t)$ is for learning efficiency based on following off-line analysis. I assessed explaining performance of various variable to the the force estimation error for using linear approximation function

$$y_i = \boldsymbol{X}\boldsymbol{\beta}, \tag{22}$$

where y_i and $\boldsymbol{X}$ are objective valiable and matrix of explaining valiable, and $\boldsymbol{\beta}$ is a paremeter vector. y_i means estimation error that was obtained from difference between the force estimated from user's biological signals $f_{est\ i}$ and the force which measured for the validation purpose by the force sensor $f_{sens\ i}$ during the three-dimensional cooperative task without the learning. Table 2 is shown the comparison of approximation performance (adjusted coefficient of determination, cf., Appendix C) of each measured valiable. Using only $\boldsymbol{m}(t)$ already requires nine learning parameters for each direction, and thus 27 parameters are required in total. I selected $\boldsymbol{m}(t)$ among many candidates including the joint angle of the robot, the hand tip motion of the user, and their delayed signals, because it gave the largest coefficient of determination responsible for linearly explaining the force estimation error. For this off-line analysis, I used the validation data described in 2, so the force estimation error was available.

Finally, the parameters α_p and β for GARB were empirically configured to 10^{-6} and 0.99.

Table 2. Comparison of approximation performance of each measured valible

y / $\boldsymbol{X}$	y_x	y_y	y_z
$\boldsymbol{\theta}$	0.3309	0.3701	0.1539
$\dot{\boldsymbol{\theta}}$	0.1493	0.0908	0.0440
$\ddot{\boldsymbol{\theta}}$	0.0417	0.0244	0.0395
$\boldsymbol{p}_{hand}$	0.1862	0.2831	0.0719
$\dot{\boldsymbol{p}}_{hand}$	0.0654	0.1688	0.0095
$\ddot{\boldsymbol{p}}_{hand}$	0.0182	0.0356	0.0376
$\boldsymbol{EMG}$(t)	0.2259	0.4599	0.2195
$\boldsymbol{EMG}$(t-5)	0.2223	0.4591	0.2217
$\boldsymbol{EMG}$(t-10)	0.2182	0.4576	0.2244
$\boldsymbol{EMG}$(t-15)	0.2145	0.4559	0.2270
$\boldsymbol{EMG}$(t-20)	0.2114	0.4538	0.2294
$\boldsymbol{EMG}$(t-25)	0.2089	0.4514	0.2315
$\boldsymbol{EMG}$(t-30)	0.2071	0.4487	0.2335

4.3.1 Results and problems

I conducted two tasks seven times (seven episodes). One episode consisted of nine trials. The desired load state $\boldsymbol{d}$ ($= [t_{\text{target}}\ x_{\text{target}}\ y_{\text{target}}\ z_{\text{target}}]^T$) was $[2.0\ 0.2\ 0.0\ 0.0]^T$ and $[2.0\ 0.0\ 0.0\ 0.2]^T$ in Task 1 and Task 2, respectively. In each trial, the task was terminated in 2.5 [s].

Figure 24 and 25 present experimental results of Tasks 1 and 2, respectively. Figure 24(a) and 25(a) show the mean and standard deviation of the accumulated reward, while Figure 24(b) and 25(b) show the reaching position error of the load. Both results were obtained over seven trials. As shown in these figures, policy gradient learning of each task was quickly accomplished. The learning speed was particularly fast in Task 2, and 24(b) and 25(b) suggest Task 2 was easier than Task 1. The panel 25(b) shows the reaching error position in the z-axis was achieved from the beginning trial, and the reaching position in the x-axis was also almost achieved. Therefore, learning was only necessary for the y-axis, and the position errors nicely decreased over trials. In contrast, the panel 24(b) shows that, in Task 1, all three reaching positions moved over

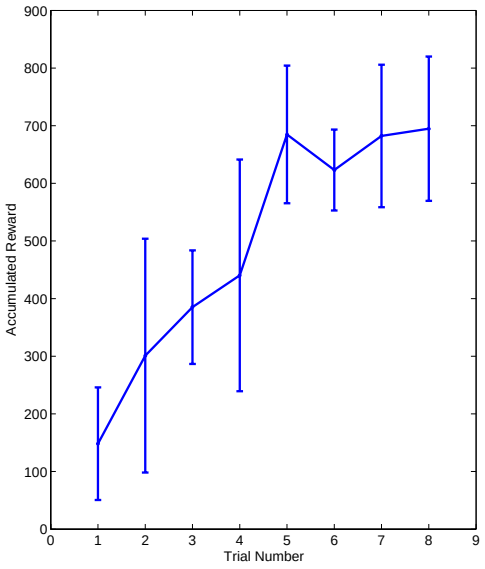

(a) Learning curve

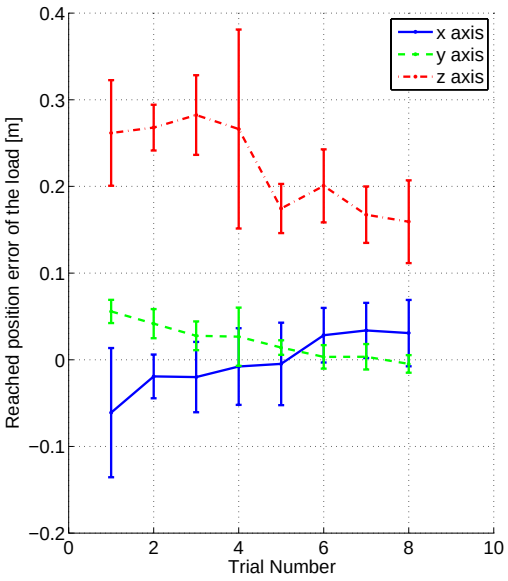

(b) Reaching position error of the load

Figure 24. Experimental results obtained in task 1

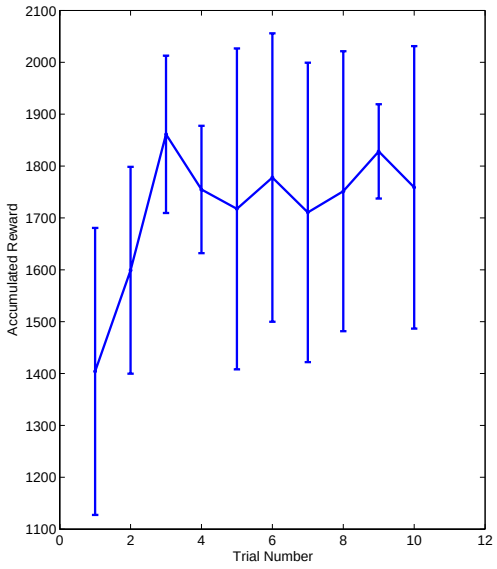

(a) Learning curve

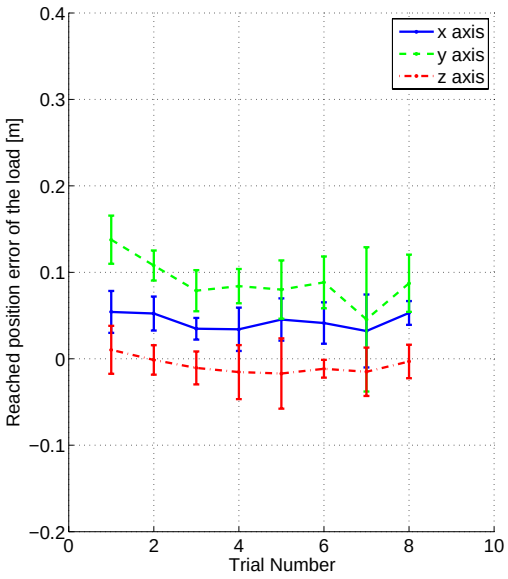

(b) Reaching position error of the load

Figure 25. Experimental results obtained in task 2

trials. The position of x-axis started from the position lower than the goal and ended around the goal. The position of y-axis started from the position higher than zero, became decreased, and ended around the goal, zero. The position of z-axis started from a very high position, then lower, and ended at a much lower position but it was still much higher than zero.

For learning, I selected only the current EMG signals as the agent's state among 256 possible states. There are two reasons why I selected the current EMG signals. First, it was for learning efficiency; the selection restricted the number of learning parameters to 27 only. Second, the current EMG signals were expected to reduce the force estimation error based on the off-line analysis. However, because corresponding terms other than the current EMG made a large contribution to the force estimation, using the current EMG terms did not work perfectly. Furthermore it is difficult to use all the terms of EMG, since there were too many parameters for efficient learning.

4.4 Experiment2: learning based on force estimation using delay-filtered EMG

To cope with the problem described above, I introduced a process of transforming EMG to muscle activation (force) for the estimation of the force applied to the user's hand in place of EMG delay-line. There is a time delay between the onset of electrical activity and exerting tension. Because it can be vary according to muscle contraction velocity and force [12, 14], I have to achive a suitable time delay between the onset of the EMG and the force. Thelen et al., modeled the relation ship between EMG and muscle activation with linear discrete time dynamic model [66]. Zajac et al., used first-order recursive differential filter for transforming to muscle activation [72], and Manal et al., proposed second-order model which works more efficiently [45, 43, 7]. I employed the second-order filter to obtain muscle activation $u_j(t)$ given by:

$$u_j = \alpha e_j(t-d) - \beta_1 u_j(t-1) - \beta_2 u_j(t-2), \tag{23}$$

where $e_j(t)$ is full-wave rectified and low-pass filtered EMG of muscle j at time t. α, β_1 and β_2 are recursive coefficients, and d is the electromechanical delay. To guarantee

the filter stability of Equation (23), constraint conditions of α, β_1 and β_2 are neccesary:

$$\beta_1 = \gamma_1 + \gamma_2 \tag{24}$$

$$\beta_2 = \gamma_1 \cdot \gamma_2 \tag{25}$$

$$|\gamma_1| < 1 \tag{26}$$

$$|\gamma_2| < 1. \tag{27}$$

To ensure that muscle activation does not exceed 1, the following condition must be set:

$$\alpha - \beta_1 - \beta_2 = 1.0. \tag{28}$$

The parameters of this filter β_1, β_2 and d are optimized using the Matlab Optimization Toolbox to be minimize the following cost function:

$$\sum_t (\boldsymbol{f}_{\rm est} - \boldsymbol{f}_{\rm sens})^2. \tag{29}$$

where $\boldsymbol{f}_{\rm sens}$ is the measured force by a force sensor in the calibration stage.

Using muscle activation $\boldsymbol{u}$, I redefined the force estimator (14) and the policy function (20) as following,

$$\boldsymbol{f}_{\rm est}(t) = \boldsymbol{W}^T[\boldsymbol{\theta}(t)^T, \dot{\boldsymbol{\theta}}(t)^T, \ddot{\boldsymbol{\theta}}(t)^T, \boldsymbol{u}(t)^T, \mathbf{1}^T]^T, \tag{30}$$

$$\begin{aligned} a_i \quad \sim \quad & \pi(a_i|\boldsymbol{s}, \boldsymbol{w}_i) = \mathcal{N}(a_i|\mu_i, \sigma_i), \\ & \mu_i = \sum_j^{N_{\rm EMG}} w_{ij} u_j, \\ & \sigma_i = \frac{1}{1 + \exp(-w_{i9})}, \quad (i = x, y, z), \end{aligned} \tag{31}$$

4.4.1 Results

I conducted a task five times (five episodes). One episode consisted 18 trials. The desired load state $\boldsymbol{d}$ ($= [t_{\rm target}\ x_{\rm target}\ y_{\rm target}\ z_{\rm target}]^T$) was $[2.0\ 0.2\ 0.0\ 0.0]^T$. In each trial, the task was terminated in 2.5 [s].

4.3

Figure 26 presents experimental results. Figure 26(a) show mean and standard

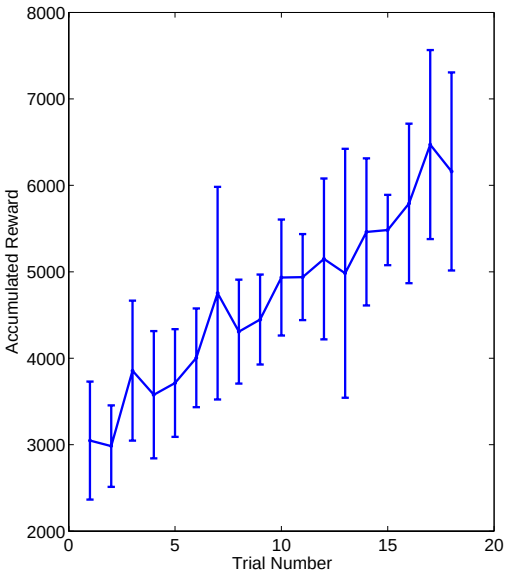

(a) Learning curve

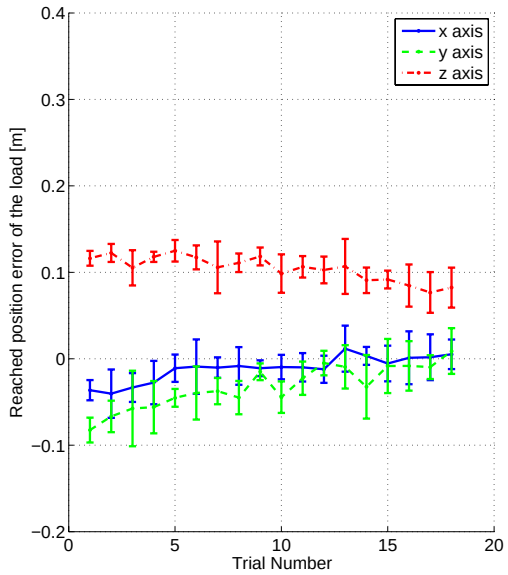

(b) Reaching position error of the load

Figure 26. Experimental results

deviation of the accumulated reward, Figure 26(b) show reaching position error of the load. As shown in this figure, the performance was improved than result in 4.3.1 by combining the terms which correspond to the EMG, however, the position of z-axis was not yet perfect. Because $\boldsymbol{\theta}$ had large contribution for the force estimation, not only EMG terms but also $\boldsymbol{\theta}$ terms should be adjusted.

4.5 Discussion

In this section, I proposed an approach to the realization of a robot controller which can adapt to changes in the muscle coordination of a user. More specifically, in this study, a three-dimensional cooperative holding task was attempted based on the virtual force sensing approach [63] in 3.4, and then its performance was improved by a policy gradient learning method. The estimation of the applied force to the user's hand that was required for this task was achieved by linear function approximation from the motion and EMG signals of the user's upper-limb. I found that this simple linear estimation worked well, even for test data, in the calibration phase. I also found, however, that it did not work in the actual task, probably due to two major reasons: (1) EMG patterns were different between in the calibration stage compared to those in the actual task, (2) the muscle coordination varied, e.g., it is known that many muscles contribute to shoulder motion, and that the torque vector of each muscle changes dramatically depending on the shoulder posture [71, 9]. I then introduced a policy gradient learning method, which is a type of reinforcement learning method, as it has the possibility of making the robot controller cope with the changes in the EMG pattern and the muscle coordination in an on-line fashion without an explicit teacher signal, i.e., measured force data. As a consequence, the goal shared by the user and the computer agent as a reward function was quickly and stably achieved in the two learning tasks. We found, however, that the performance was not yet perfect in Task 1, particularly along the z-axis. By looking into the recorded data, it seems that activated muscles were overlapped both in the x-axis and in the z-axis. In Task 2 where the x-position of the load should be zero, the result showed no interference occurred in movements towards the z-axis and the x-axis. Therefore, there would be interference created by the movement towards the x-axis with the estimation of the force along the z-axis. The resolution of this problem is planned in future studies.

Note that, as stated in 2, my approach is not confined to the cooperative holding

task. Application of my approach to other tasks such as motor learning and rehabilitation is also planned for future work.

5. Conclusion

5.1 Summary

In this dissertation, I first proposed a new approach to designing intelligent machines that can work for humans not only in industrial factories but also in my daily life such as at home. The key of the approach is the virtual realization of force/tactile sensors in robots by using user's biological signals such as EMG and postural information. In principle because my approach does not require the sensors to be attached to a robot, it can be applied not only to robots but also to various other machines. It is notable that my approach is not confined to what I call "robots", but rather it should be useful for various intelligent machine applications as mentioned in Section 2.2. My approach will become more advantageous especially with the advent of ubiquitous computing environments in which sensors and devices are networked and are distributed over the environment.

I tried a three-dimensional cooperative holding task based on the virtual force sensing approach in 3.4, however, the calibration method in which the parameters of the estimator are learned before the actual task did not work due to the variation of EMG signals attributed to time varying muscle coordination patterns.

Therefore, in this study, I introduced reinforcement learning which modified the policy function based on the user's biological signals. This can make the robot controller adaptive to the changes in the EMG pattern and the muscle coordination in an on-line fashion, without an explicit teacher signal, e.g., force sensor output, and thus we can conduct experiments in which a subject moves a heavy load to a specified target point cooperatively with a robot. Experimental results demonstrate the feasibility of my method.

5.2 Future Works

If the number of sensors, attached to the user in an unorganized manner, increases, the user would feel uncomfortable. Glove-like devices in which cheap inertial and positional sensors and electrodes for EMG are attached in an organized manner could resolve the above issue My future work will take more muscles and more sensor devices into account for more precise and robust force estimation. I am also interested in the

estimation of various internal states of humans, such as impedance of arms, with the ultimate intention of assisting cooperative tasks [29]. My long-term goal is to achieve full-body cooperation between a humanoid robot and its user based on the measurement of the full-body muscles of the user, and possibly on the ”internal” intentions of the user.

Reinforcement learning based on a user's biological signals is expected to have applications in motor learning assist-systems that will adaptively assist according to the user's intention or ability.

Acknowledgements

研究活動全般にわたって熱心にご指導下さった柴田智広准教授，池田和司教授，石井信教授，小笠原司に深く感謝致します．PA10 の制御に関して助言を頂いた本学システム制御・管理講座の中村文一助教に感謝致します．また，ロボティクス講座の池田篤俊さん，近藤誠宏博士（現 任天堂），丁明さんには当講座の実験機器が不調の際に助けて頂き，ありがとうございました．

References

[1] P. K. Artemiadis and K. J. Kyriakopoulos. EMG-based position and force control of a robot arm: Application to teleoperation and orthosis. In *Proc IEEE/ASME Int Conf Adv Intell Mechatron*, pages 1–6, 2007.

[2] M. Asghari Oskoei and H. Hu. Myoelectric control systems?A survey. *Biomedical Signal Processing and Control*, 2(4):275–294, 2007.

[3] E.R. Bachmann, X. Yun, and R.B. McGhee. Sourceless tracking of human posture using small inertial/magnetic sensors. In *Proc IEEE Int Symp on Comp Intell in Robotics and Autom*, volume 2, pages 822– 829, 2003.

[4] J.V. Basmajian. *Muscles Alive, Their Functions Revealed by Electromyography*. Williams \& Wilkins, 1978.

[5] R.E. Bellman. A Markov decision process. *Journal of Mathematical Mechanics*, 6:679–684, 1957.

[6] F. Billaut, F.A. Basset, and G. Falgairette. Muscle coordination changes during intermittent cycling sprints. *Neuroscience Letters*, 380(3):265–269, 2005.

[7] T.S. Buchanan, D.G. Lloyd, K. Manal, and T.F. Besier. Neuromusculoskeletal Modeling: Estimation of Muscle Forces and Joint Moments and Movements From Measurements of Neural Command. *Journal of applied biomechanics*, 20(4):367, 2004.

[8] TS Buchanan, MJ Moniz, JP Dewald, and R.W. Zev. Estimation of muscle forces about the wrist joint during isometric tasks using an EMG coefficient method. *J Biomech*, 26(4-5):547–60, 1993.

[9] CA. Buneo, JF. Soechting, and M. Flanders. Postural dependence of muscle actions: Implications for neural control. *J. Neurosci.*, 17(6):2128–2142, 1997.

[10] I. Campanini, A. Merlo, P. Degola, R. Merletti, G. Vezzosi, and D. Farina. Effect of electrode location on EMG signal envelope in leg muscles during gait. *Journal of Electromyography and Kinesiology*, 17(4):515–526, 2007.

[11] E.E. Cavallaro, J. Rosen, J.C. Perry, and S. Burns. Real-time myoprocessors for a neural controlled powered exoskeleton arm. *IEEE Trans Biomed Eng*, 53(11):2387–2396, 2006.

[12] PR Cavanagh and PV Komi. Electromechanical delay in human skeletal muscle under concentric and eccentric contractions. *European Journal of Applied Physiology*, 42(3):159–163, 1979.

[13] JH CHALLIS and DG KERWIN. Determining individual muscle forces during maximal activity: model development, parameter determination, and validation. *Human movement science*, 13(1):29–61, 1994.

[14] DM. Corcos, GL. Gottlieb, ML. Latash, GL. Almeida, and GC. Agarwal. Electromechanical delay: An experimental artifact. *J Electromyogr Kinesiol*, 2:59–68, 1992.

[15] C.J. De Luca. The Use of Surface Electromyography in Biomechanics. *JOURNAL OF APPLIED BIOMECHANICS*, 13:135–163, 1997.

[16] Catherine Disselhorst-Klug, Thomas Schmitz-Rode, and Gunter Rau. Surface electromyography and muscle force: Limits in semg-force relationship and new approaches for applications. *Clinical Biomechanics*, In Press, Corrected Proof:–, 2008.

[17] A. Dutta and G. Obinata. Impedance control of a robotic gripper for cooperation with humans. *Control Engineering Practice*, 10(4):379–389, 2002.

[18] A. EBERSTEIN. SIMULTANEOUS MEASUREMENT OF MUSCLE CONDUCTION VELOClITY AND EMG POWER SPECTRUM CHANGES DURING FATIGUE. *MUSCLE \& NERVE*, 3:788–773, 1985.

[19] A. Erdemir, S. McLean, W. Herzog, and A.J. van den Bogert. Model-based estimation of muscle forces exerted during movements. *Clinical Biomechanics*, 22(2):131–154, 2007.

[20] D. Farina, R. Merletti, and R.M. Enoka. The extraction of neural strategies from the surface EMG, 2004.

[21] C. Fleischer, C. Reinicke, and G. Hommel. Predicting the intended motion with EMG signals for an exoskeleton orthosis controller. In *Intelligent Robots and Systems, 2005.(IROS 2005). 2005 IEEE/RSJ International Conference on*, pages 2029–2034, 2005.

[22] A.J. Fridlund and J.T. Cacioppo. Guidelines for Human Electromyographic Research. *Psychophysiology*, 23(5):567–589, 1986.

[23] O. Fukuda, T. Tsuji, M. Kaneko, and A. Otsuka. A human-assisting manipulator teleoperated by EMG signals and arm motions. *IEEE Trans Robot Automat*, 19(2):210–222, 2003.

[24] A. Gallagher, Y. Matsuoka, and Wei-Tech Ang. An efficient real-time human posture tracking algorithm using low-cost inertial and magnetic sensors. In *Proc IEEE Int Conf Intell Robot Syst*, volume 3, pages 2967–2972, 2004.

[25] AV Hill. The Heat of Shortening and the Dynamic Constants of Muscle. *Proceedings of the Royal Society of London. Series B, Biological Sciences*, 126(843):136–195, 1938.

[26] T. Hoshi and H. Shinoda. A tactile sensing element for a whole body robot skin. In *Proc 12th Int Symp Robot Res (CD-ROM)*, 2005.

[27] B. Hudgins, P. Parker, and RN Scott. A new strategy for multifunction myoelectric control. *Biomedical Engineering, IEEE Transactions on*, 40(1):82–94, 1993.

[28] T. Iberall, G. Sukhatme, D. Beattie, and Bekey G. On the development of EMG control for a prosthesis using a robotic hand. In *Proc IEEE Int Conf Robot Automat*, pages 1753–1758, 1994.

[29] R. Ikeura, H. Inooka, and K. Mizutani. Subjective evaluation for maneuverability of a robot cooperating with humans. *J. Robot Mechatron*, 14(5):514–519, 2002.

[30] K. Irie, N. Wakamura, and K. Umeda. Construction of an intelligent room based on gesture recognition: operation of electric appliances with hand gestures. In *Proc IEEE Int Conf Intell Robot Syst*, volume 1, pages 193–198, 2004.

[31] H. Ishiguro. Distributed vision system: a perceptual information infrastructure for robot navigation. In *Proc the Fifteenth Int Joint Conf on Artif Intell*, volume 1, pages 36–41, 1997.

[32] H. Kawamoto and Y. Sankai. Quantitative motion control analysis method for power assist system based on human motion property. *Trans JSME ser C*, 70(692):1115–1123, 2004.

[33] Y. Koike, K. Honda, M. Hirayama, H. Gomi, E. Bateson, and M. Kawato. Estimation of isometric torques from surface electromyography using a neural network model. *IEICE Trans*, J76-D-II(6):1270–1279, 1993.

[34] Y. Koike and M. Kawato. Trajectory formation from surface EMG signals using a neural network model. *IEICE Trans*, J77-D-II(1):193–203, 1994.

[35] Y. Koike and M. Kawato. Estimation of dynamic joint torques and trajectory formation from surface electromyography signals using a neural network model. *Biol Cybern*, 73(4):291–300, 1995.

[36] P.V. Komi and P. Tesch. EMG frequency spectrum, muscle structure, and fatigue during dynamic contractions in man. *European Journal of Applied Physiology*, 42(1):41–50, 1979.

[37] J. Langenderfer, S. LaScalza, A. Mell, J.E. Carpenter, J.E. Kuhn, and R.E. Hughes. An EMG-driven model of the upper extremity and estimation of long head biceps force. *Computers in Biology and Medicine*, 35(1):25–39, 2005.

[38] M.L. Latash. *Neurophysiological Basis of Movement*. Human Kinetics Publishers, Inc., 1998.

[39] WA Lee, TS Buchanan, and MW Rogers. Effects of arm acceleration and behavioral conditions on the organization of postural adjustments during arm flexion. *Experimental Brain Research*, 66(2):257–270, 1987.

[40] M.A. Lemay and P.E. Crago. A dynamic model for simulating movements of the elbow, forearm, and wrist. *Journal of Biomechanics*, 29(10):1319–1330, 1996.

[41] L. Li and B.S. Baum. Electromechanical delay estimated by using electromyography during cycling at different pedaling frequencies. *Journal of Electromyography and Kinesiology*, 14(6):647–652, 2004.

[42] MM Liu, W. Herzog, and HH Savelberg. Dynamic muscle force predictions from EMG: an artificial neural network approach. *J Electromyogr Kinesiol*, 9(6):391–400, 1999.

[43] D.G. Lloyd and T.F. Besier. An EMG-driven musculoskeletal model to estimate muscle forces and knee joint moments in vivo. *Journal of Biomechanics*, 36(6):765–776, 2003.

[44] JJ Luh, GC Chang, CK Cheng, JS Lai, and TS Kuo. Isokinetic elbow joint torques estimation from surface EMG and joint kinematic data: using an artificial neural network model. *J Electromyogr Kinesiol*, 9(3):173–83, 1999.

[45] K. Manal, R.V. Gonzalez, D.G. Lloyd, and T.S. Buchanan. A real-time EMG-driven virtual arm. *Computers in Biology and Medicine*, 32(1):25–36, 2002.

[46] S.A. Mascaro and H.H. Asada. Measurement of finger posture and three-axis fingertip touch force using fingernail sensors. *IEEE Trans Robot Automat*, 20(1):26–35, 2004.

[47] R. Merletti and P. Parker. *Electromyography: Physiology, Engineering, and Non-invasive Applications*. Wiley-IEEE Press, 2004.

[48] N. Mitsunaga, C. Smith, T. Kanda, H. Ishiguro, and N. Hagita. Adapting robot behavior for human-robot interaction. *IEEE Trans Robot*, 24(4):911–916, 2008.

[49] T. Miyashita, T. Tajika, H. Ishiguro, K. Kogure, and N. Hagita. Haptic communication between humans and robots. In *Proc 12th Int Symp Robot Res (CD-ROM)*, 2005.

[50] T. Mori, H. Noguchi, A. Takaga, and T. Sato. Sensing room: Distributed sensor environment for measurement of human daily behavior. In *Proc 1st Int Workshop Networked Sensing Syst*, pages 40–43, 2004.

[51] S. Morinaga and K. Kosuge. Compliant motion control of manipulator's redundant dof based on model-based collision detection system. In *Proc IEEE Int Conf Robot Automat*, pages 5212–5217, 2004.

[52] H. Morishita, Y. Kosaka, N. Hosoda, K. Ohgushi, T. Yamanishi, M. Hosseinbor, K. Watanabe, R. Fukui, T. Kobayashi, S. Shiotani, Y. Majima, T. Kuroiwa, T. Fujimoto, H. Noguchi, T. Mori, and T. Sato. Realization of hyper-robot system: A robotically supported room environment in 2020. In *Proc Int Symp on Robot*, page TU4H2, 2005.

[53] M. Naeije and H. Zorn. Relation between EMG power spectrum shifts and muscle fibre action potential conduction velocity changes during local muscular fatigue in man. *European Journal of Applied Physiology*, 50(1):23–33, 1982.

[54] H. Ogino, J. Arita, and T. Tsuji. A wearable pointing device using EMG signals. *J. Robot Mechatron*, 17(2):173–180, 2005.

[55] A. Pedotti, P. Crenna, A. Deat, C. Frigo, and J. Massion. Postural synergies in axial movements: short and long-term adaptation. *Experimental Brain Research*, 74(1):3–10, 1989.

[56] MBI Raez, MS Hussain, and F. Mohd-Yasin. Techniques of EMG signal analysis: detection, processing, classification and applications. *Biological Procedures Online*, 8(1):11–35, 2006.

[57] Jacob Rosen, Moshe B. Fuchs, and Mircea Arcan. Performances of hill-type and neural network muscle models–toward a myosignal-based exoskeleton. *Computers and Biomedical Research*, 32(5):415 – 439, 1999.

[58] D. Rumelhart, G. Hinton, and R. Williams. Learning representations by back-propagating errors. *Nature*, 325:533–536, 1986.

[59] T. Sadoyama, T. Masuda, and H. Miyano. Relationships between muscle fibre conduction velocity and frequency parameters of surface EMG during sustained contraction. *European Journal of Applied Physiology*, 51(2):247–256, 1983.

[60] DF Stegeman, JH Blok, HJ Hermens, and K. Roeleveld. Surface EMG models: properties and applications. *J Electromyogr Kinesiol*, 10(5):313–26, 2000.

[61] R.S. Sutton and A.G. Barto. *Reinforcement Learning: An Introduction*. MIT Press, 1998.

[62] S. Tachi, T. Sakaki, H. Arai, S. Nishizawa, and J. Pelaez-polo. Impedance control of a direct drive manipulater without using force snsors. *J. of Robot Soc of Jpn*, 7(3):60–72, 1989.

[63] T. Tamei, S. Ishii, and T. Shibata. Virtual force/tactile sensors for interactive machines using the user's biological signals. *Adv. Robot.*, 22(8):893–911, 2008.

[64] Y. Tao, H. Hu, and H. Zhou. Integration of vision and inertial sensors for 3D arm motion tracking in home-based rehabilitation. *Int J. Robotics Research*, 26(6):607–624, 2007.

[65] A. Tapus, C. Tapus, and M.J. Mataric. Hands-off therapist robot behavior adaptation to user personality for post-stroke rehabilitation therapy. In *Proc IEEE Int Conf Robot Automat*, pages 1547–1553, 2007.

[66] DG Thelen, AB Schultz, SD Fassois, and JA Ashton-Miller. Identification of dynamic myoelectric signal-to-force models during isometric lumbar muscle contractions. *J Biomech*, 27(7):907–19, 1994.

[67] N. Tsujiuchi, T. Koizumi, and M. Yoneda. Manipulation of a robot by EMG signals using linear multiple regression model. In *Proc IEEE Int Conf Intell Robot Syst*, pages 1991–1996, 2004.

[68] L. Weaver and N. Tao. The optimal reward baseline for gradient-based reinforcement learning. In *Proc 17th Conf Uncertainty in Artificial Intelligence*, pages 538–545, 2001.

[69] J.M. Winters and L. Stark. Muscle models: What is gained and what is lost by varying model complexity. *Biological Cybernetics*, 55(6):403–420, 1987.

[70] JF Yang and DA Winter. Electromyographic amplitude normalization methods: improving their sensitivity as diagnostic tools in gait analysis. *Arch Phys Med Rehabil*, 65(9):517–21, 1984.

[71] N. Yoshida, K. Domen, Y. Koike, and M. Kawato. A method for estimating torque-vector directions of shoulder muscles using surface EMGs. *Bio. Cybern.*, 86(3):167–177, 2002.

[72] FE Zajac. Muscle and tendon: properties, models, scaling, and application to biomechanics and motor control. *Crit Rev Biomed Eng*, 17(4):359–411, 1989.

[73] V. Zatsiorsky and V. Seluyanov. The mass and inertia characteristics of the main segments of the human body. *Biomechanics*, VIII-B:1152–1159, 1983.

[74] M. Zecca, S. Micera, MC Carrozza, and P. Dario. Control of Multifunctional Prosthetic Hands by Processing the Electromyographic Signal. *CRITICAL REVIEWS IN BIOMEDICAL ENGINEERING*, 30(4/6):459–485, 2002.

[75] 木塚朝博, 増田正, 木竜徹, and 佐渡山亜兵共. **表面筋電図**. 東京電機大学出版局, 東京, 2006.

Appendix

A. Estimation of the three-dimensional force-vector bearing on the hand based on forward dynamics

The dynamic balancing between the force and the torque on every link can be described by the Newton-Euler formulation. The backward recursive equation for dynamics are,

$$\boldsymbol{f}_i = \boldsymbol{A}_{i+1}\boldsymbol{f}_{i+1} + m_i\ddot{\boldsymbol{p}}_{gi}, \tag{32}$$

$$\boldsymbol{n}_i = \boldsymbol{A}_{i+1}\boldsymbol{n}_{i+1} + \boldsymbol{I}_i\dot{\boldsymbol{\omega}}_i + \boldsymbol{\omega}_i \times (\boldsymbol{I}_i\boldsymbol{\omega}_i) + \boldsymbol{a}_i \times (m_i\ddot{\boldsymbol{p}}_{gi}) + \boldsymbol{l}_i \times \boldsymbol{A}_{i+1}\boldsymbol{f}_{i+1}, \tag{33}$$

$$\tau_i = \boldsymbol{q}_i^T\boldsymbol{n}_i + D_i\dot{\theta}_i + E_i(\dot{\theta}_i, \theta_i), \tag{34}$$

$$(i = p, p-1, \cdots, 1),$$

where, $\boldsymbol{A}_i$, $\boldsymbol{I}_i$, $\boldsymbol{\omega}_i$, $\boldsymbol{a}_i$, m_i, $\boldsymbol{p}_{gi}$, $\boldsymbol{l}_i$, $\boldsymbol{f}_i$ and $\boldsymbol{n}_i$ are a coordinate transformation matrix from the $(i-1)$-th to the i-th coordinate systems, an inertia matrix on the gravity center of the i-th link, an angular velocity vector of the i-th link, a vector from the origin to the gravity center of the ith link, a mass of the i-th link, a vector from the world origin to the gravity center of the tip link, a vector from the origin of the i-th link to the origin of the $(i+1)$-th link, and a force vector which acts on the i-th link from the $(i-1)$-th link, and a moment vector for the i-th link from the $(i-1)$-th link, respectively. $\boldsymbol{q}_i$ is the vector denoting the rotational axis and only a element is 1. D_i and $E_i(\dot{\theta}_i, \theta_i)$ are the viscous friction coefficient for the joint and the nonlinear friction torque, respectively, and they were set at 0 for simplicity. p is the number of the links. Although the purpose is calculating the force vector which acts on the tip link $\boldsymbol{f}_{p+1}$, it could not be derived analytically, so corss product in (33) has no unique inverse.

Therefore, I obtained $\boldsymbol{f}_{p+1}$ numerically by expanding (32), (33) as following,

$$\boldsymbol{f}_i = \begin{pmatrix} F_{11}^{\ i} & F_{12}^{\ i} & F_{13}^{\ i} & F_{14}^{\ i} \\ F_{21}^{\ i} & F_{22}^{\ i} & F_{23}^{\ i} & F_{24}^{\ i} \\ F_{31}^{\ i} & F_{32}^{\ i} & F_{33}^{\ i} & F_{34}^{\ i} \end{pmatrix} \begin{pmatrix} f_x^{\ p+1} \\ f_y^{\ p+1} \\ f_z^{\ p+1} \\ 1 \end{pmatrix}, \tag{35}$$

$$\boldsymbol{n}_i = \begin{pmatrix} N_{11}^{\ i} & N_{12}^{\ i} & N_{13}^{\ i} & N_{14}^{\ i} \\ N_{21}^{\ i} & N_{22}^{\ i} & N_{23}^{\ i} & N_{24}^{\ i} \\ N_{31}^{\ i} & N_{32}^{\ i} & N_{33}^{\ i} & N_{34}^{\ i} \end{pmatrix} \begin{pmatrix} f_x^{\ p+1} \\ f_y^{\ p+1} \\ f_z^{\ p+1} \\ 1 \end{pmatrix}. \tag{36}$$

The relationship between τ_i and matrix N^i is specified by using (34), because only one of elements of $\boldsymbol{q}_i$ is 1.

B. GPOMDP Algorithm

(1) The agent observed the state $\boldsymbol{s_t}$ from the environment and take action $\boldsymbol{a_t}$ based on probabilistic policy $\pi(\boldsymbol{a_t}, \boldsymbol{s_t}, \boldsymbol{w(t)})$,
(2) is given reward r_t and observed the next state $\boldsymbol{s_{t+1}}$.
(3) update action selection probability

$$\begin{aligned} e_i(t) &= \frac{\partial}{\partial w_i(t)} \ln\left(\pi(\boldsymbol{a_t}, \boldsymbol{s_t}, \boldsymbol{w}(t))\right) \\ D_i(t) &= e_i(t) + \beta D_i(t) \\ b(t) &= b(t-1) + \frac{1}{t}(r(t) - b(t-1)) \\ \Delta w_i(t) &= (r(t) - b(t)) \\ \boldsymbol{w}(t+1) &= \boldsymbol{w(t)} + \alpha_p \Delta \boldsymbol{w}(t) \end{aligned}$$

$e_i(t)$ and $D_i(t)$ are eligibility and eligibility trace. $\boldsymbol{w}(t) = (w_1(t), w_2(t), \cdots, w_l(t))$ is parameters. β $(0 < \beta < 1)$ and α_p are discount ratio of eligibility trace and learning ratio, respectively.
(4) set a time t forward and return to step (1).

C. Adjusted Coefficient of Determination

Adjusted coefficient of determination $\bar{R}^2$ is given by following equations

$$R^2 = \frac{\sum_{t=1}^{n}(\hat{y}(t) - \bar{y})^2}{\sum_{t=1}^{n}(y(t) - \bar{y})^2} = 1 - \frac{\sum_{t=1}^{n} e(t)^2}{\sum_{t=1}^{n}(y(t) - \bar{y})^2}, \tag{37}$$

$$\bar{R}^2 = 1 - \frac{n-1}{n-p-1}(1 - R^2). \tag{38}$$

$\hat{\boldsymbol{y}}$ and $\bar{y}$ are predictive vector and average of objective variable. n and p are number of samples and parameters of explaining variable, respectively. $\boldsymbol{e}$ is residual vector that calculated by

$$\boldsymbol{e} = \boldsymbol{y} - \hat{\boldsymbol{y}}.$$

Publications

Journal Papers

1. **Tomoya Tamei**, Shin Ishii and Tomohiro Shibata
   Virtual Force/Tactile Sensors for Interactive Machines Using User's Biological Signals
   Advanced Robotics, 22(8), 893-911, 2008.

2. **Tomoya Tamei** and Tomohiro Shibata
   Reinforcement Learning of the Virtual Force Sensing for Kinetic Human-Robot Cooperation
   Autonomous Robots, submitted.

Conference Proceedings (reviewed)

1. **Tomoya Tamei** and Tomohiro Shibata
   Policy Gradient Learning of Cooperative Interaction with a Robot Using User's Biological Signals
   International Conference on Neural Information Processing (ICONIP 2008), to appear.

2. **Tomoya Tamei**, Shin Ishii and Tomohiro Shibata
   Dynamic and Cooperative Interaction with a Robot that Possesses No Force/Tactile Sensors
   International Conference Advanced Robotics (ICAR 2007), pp.647-652, 2007.

3. **Tomoya Tamei**, Tomohiro Shibata and Shin Ishii
   Development of learning support system for piano-keying -Relationship between the activity of finger muscles and key release velocities of an expert-
   International Symposium on Artificial Life and Robotics (AROB 11th '06), GS7-5, 2006.

4. Tomohiro Nomura, Tomohiro Shibata, **Tomoya Tamei** and Shin Ishii
   Extended force/tactile senses of machines by measurement of user's biological signals
   36th International Symposium on Robotics (ISR 2005), CD-ROM, 2005.

Conference Proceedings

1. **Tomoya Tamei**, Shin Ishii and Tomohiro Shibata
   Virtual Force/Tactile Sensors for Dynamic and Cooperative Interaction with a

Robot Using User's Biological Signals
Neuro2007, 2007.

2. **為井 智也**, 石井 信 柴田 智広
ユーザーの生体信号計測に基づいたロボットとの動的・協調的インタラクション
電子情報通信学会技術研究報告 NC ニューロコンピューティング, 107(50), pp.9-14, 2007.

3. **為井 智也**, 石井 信 柴田 智広
筋電信号に基づいた示指によるピアノ打鍵時の脱力度評価
情報処理学会研究報告, 音楽情報科学研究会, 2005-MUS-61, pp.47-52, 2005.

Other

1. 2007 年度 （財）三井住友海上福祉財団研究助成.